TRENDS IN SCIENCES 2026; 23(12): 14186
https://doi.org/10.48048/tis.2026.14186 RESEARCH ARTICLE

Hepatoprotective and Anti-Inflammatory Effects of the As-Capsipol Complex: An Integrated *In Vivo* and *In Silico* Study

Ibragim Raxmanovich Askarov[2], Baxtigul Obidova Ro'zmat Qizi[1,*], Surayyo Mamatqulova Abdusamatovna[3] and Muzaffar Obidov[4]

[1]*Department of Technological Machines and Equipment, Fergana State Technical University, Uzbekistan*
[2]*Department of Chemistry, Tabobat" Academy of Uzbekistan, Tashkent, Uzbekistan*
[3]*Department of Chemistry, Fergana State University, Uzbekistan*
[4]*Department of Zoology and General Biology, Fergana State University, Uzbekistan*

([*]Corresponding author's e-mail: baxtigulobidova@gmail.com)

Received: 24 April 2026, Revised: 25 May 2026, Accepted: 4 June 25, 2026, Published: 30 July 2026

Abstract

This study investigated the hepatoprotective, anti-inflammatory, and safety properties of the As-Capsipol complex using combined *in vivo* and *in silico* approaches. Acute liver injury was induced in rats by administration of a toxic dose of paracetamol, resulting in significant hepatocellular damage, as evidenced by increased alanine aminotransferase (ALT) and aspartate aminotransferase (AST) levels and decreased blood urea concentration. Treatment with As-Capsipol at 150 mg/kg for 14 days improved these biochemical parameters, including reduction of transaminase activity and partial restoration of urea levels, suggesting recovery of liver function. Anti-inflammatory activity was evaluated using a carrageenan-induced paw edema model. As-Capsipol exhibited dose-dependent anti-exudative effects, with the highest activity observed at 150 mg/kg, indicating attenuation of acute inflammatory responses. Acute toxicity testing in mice showed no mortality or persistent adverse effects at a dose of 2,000 mg/kg, suggesting low acute toxicity under the tested conditions. To investigate potential mechanisms, molecular docking studies were conducted against key inflammation-related targets, including MAPK, NF-kB, and TNF-α. The selected amino acids demonstrated binding energies ranging from −5.0 to −8.1 kcal/mol. The binding affinity pattern followed the order: Tryptophan > tyrosine ≈ phenylalanine > arginine > glutamic acid, indicating stronger interactions for aromatic amino acids. These interactions were stabilized by hydrogen bonding and hydrophobic contacts within protein active sites. The findings indicate that As-Capsipol may support liver function and modulate inflammatory processes under experimental conditions. Further studies are required to confirm these effects and clarify the underlying mechanisms.

Keywords: As-Capsipol, Hepatoprotective activity, Molecular docking, MAPK, NF-kB, TNF-α, Paracetamol-Induced hepatitis

Introduction

Liver diseases remain a major global health concern due to their increasing prevalence and complex pathophysiology. Among experimental models, paracetamol-induced hepatotoxicity is widely used to study acute liver injury, as it closely mimics clinical conditions associated with oxidative stress and hepatocellular damage. The toxic effects of paracetamol are primarily mediated by the formation of the reactive metabolite N-acetyl-p-benzoquinone imine (NAPQI), which leads to depletion of intracellular glutathione, disruption of mitochondrial function, and subsequent hepatocyte necrosis [1]. In addition to oxidative stress, inflammatory processes play a critical role in the progression of liver injury. Activation of key signaling pathways, including mitogen-activated protein kinases (MAPK), nuclear factor kappa B (NF-kB), and tumor necrosis factor-alpha (TNF-α), contributes to the

amplification of inflammatory responses and further aggravation of tissue damage. Therefore, compounds capable of modulating both oxidative and inflammatory mechanisms are of particular interest in the development of hepatoprotective agents [2]. Natural products and biologically active complexes derived from medicinal plants have attracted considerable attention due to their multifunctional properties and relatively favorable safety profiles. In this context, the As-Capsipol complex, obtained from *Polygonum aviculare* L. and *Capsicum annuum* L., represents a promising candidate. This complex contains a diverse range of bioactive components, including amino acids, which may contribute to its biological activity through antioxidant and anti-inflammatory mechanisms [3]. Recent advances in computational methods, particularly molecular docking, have enabled the prediction of ligand–protein interactions and provided valuable insights into the potential mechanisms of action of biologically active compounds. The integration of *in vivo* experimental models with *in silico* approaches allows for a more comprehensive evaluation of pharmacological effects and underlying molecular interactions [4]. Based on these considerations, the present study aimed to evaluate the hepatoprotective, anti-inflammatory, and safety properties of the As-Capsipol complex using experimental models of paracetamol-induced liver injury and carrageenan-induced inflammation, complemented by molecular docking analysis targeting key inflammatory proteins, including COX-2, IL-6, MAPK, NF-kB, and TNF-α.

Materials and methods

The study was conducted using adult white outbred animals under standard laboratory conditions. All experimental procedures were performed in accordance with accepted ethical guidelines for animal research.

Acute toxicity study

The acute toxicity of the As-Capsipol complex obtained from *Polygonum aviculare* L. and *Capsicum annuum* L. was evaluated according to the OECD Guideline (2001) using the fixed-dose procedure [1]. The test substance was administered orally via gastric gavage using a specialized probe. The study was performed on male white outbred mice weighing 21.2 ± 2.0 g. Animals were acclimatized for 10 - 14 days prior to experimentation. A total of 10 animals were used, divided into 2 groups (n = 5 per group). The experiment was conducted in 2 sequential stages. In the first stage, 2 animals received a single oral dose of As-Capsipol at 2,000 mg/kg (0.4 mL). The animals were observed for 48 - 72 h, and no mortality was recorded. In the second stage, the remaining 3 animals were administered the same dose under identical conditions. A control group received an equivalent volume of distilled water (0.4 mL). During the first day, animals were monitored hourly for general condition, behavioral changes, tremors, and mortality. Further observations were carried out daily for 14 days, including assessment of locomotor activity, skin and fur condition, respiratory rate, urination, and body weight changes. Animals had free access to food and water throughout the study. At the end of the experiment, the median lethal dose (LD50) and toxicity class of As-Capsipol were estimated based on the obtained data [2,3].

Anti-inflammatory activity (carrageenan-induced paw edema model)

The anti-inflammatory activity of As-Capsipol was evaluated using the classical carrageenan-induced paw edema model. The study was conducted on 30 white outbred rats (190 ± 20 g) of the same sex. Animals were randomly divided into 5 groups (n = 6 per group): 1 control group and 4 experimental groups. Acute inflammation was induced by subplantar injection of 0.1 mL of 1% carrageenan solution into the hind paw of each animal. The test compound, As-Capsipol (a 3:1 preparation obtained from *Polygonum aviculare* L. and *Capsicum annuum* L.), was administered orally in powder form at doses of 50, 100, and 150 mg/kg, 1 h prior to carrageenan injection. The reference drug (Laksidol, 10 mg/kg) was also administered under the same conditions. The inflammatory response was assessed by measuring changes in paw volume at 1, 2, 3, and 4 h after carrageenan administration. The anti-exudative activity (AEF) was calculated based on the edema values at the 3-hour time point using the following formula:

$$AEF\ (\%) = \frac{\Delta \mathrm{Vn} - \Delta \mathrm{Vexp}}{\Delta \mathrm{Vn}} \times 100$$

where AEF represents anti-exudative activity (%), ΔVn is the paw volume in the control group, and ΔVexp is the paw volume in the treated group [2].

Paracetamol-induced acute hepatotoxicity model

The study was carried out on adult white outbred rats of both sexes, weighing 180 - 200 g. Animals were randomly assigned to experimental groups (n = 5 per group) with balanced sex distribution to minimize potential bias. Acute toxic hepatitis was induced by oral administration of paracetamol (acetaminophen) at a dose of 150 mg/kg once daily for 2 consecutive days via gastric gavage [5]. This model is associated with oxidative stress–mediated hepatocellular injury due to depletion of antioxidant defenses. Following confirmation of hepatotoxicity, treatment was initiated. The experimental group received the AS-Capsipol compound at a dose of 150 mg/kg, while the reference group was treated with Heptral (ademetionine) at 225 mg/kg. Both treatments were administered orally once daily for 14 consecutive days. Control groups included intact (healthy) animals and a paracetamol-treated group receiving vehicle only. Animals were allocated to groups using randomization procedures, and all outcome assessments were performed under blinded conditions to reduce observer bias. The general condition of the animals, including behavior, activity, and survival, was monitored daily throughout the experimental period [6].

Serum biochemical parameters

After administration of AS-Capsipol (150 mg/kg) and the reference preparation within the defined experimental period, blood samples were collected from the venous system of the experimental animals into vacuum tubes (“HumaTubeSerum C/A”) intended for serum biochemical analysis [7]. Serum was separated by centrifugation at 3,000 rpm for 15 min. Biochemical parameters were measured using an automated analyzer (DIRUI CS-T240, Dirui Industrial Co., Ltd., China) with reagent kits from Cypress Diagnostics (Belgium). Hemolysis-free serum samples were used to determine total protein, aspartate aminotransferase (AST), alanine aminotransferase (ALT), and urea levels. Renal function was evaluated under water loading conditions (5% of body weight) by measuring 4-hour diuresis. Additional parameters included serum urea concentration (mmol/L), urine pH, and the presence of nitrites, glucose, leukocytes, and other indicators using qualitative test strips (Combina, Germany), along with microscopic examination of urinary sediment [8].

Preparation, composition and standardization of AS-Capsipol

The AS-Capsipol complex was prepared using the aerial parts of *Polygonum aviculare* L. (including stems, leaves, and flowers) and the fruits of *Capsicum annuum* L. The plant materials were collected from the Oltiariq and Rishton districts of the Fergana region, Republic of Uzbekistan. All plant samples were harvested during their appropriate vegetative period and were selected based on morphological integrity and absence of visible damage.

Kingdom: Plantae
Clade: Tracheophytes
Clade: Angiosperms
Clade: Eudicots
Order: Caryophyllales
Family: Polygonaceae
Genus: *Polygonum*
Species: *Polygonum aviculare* L

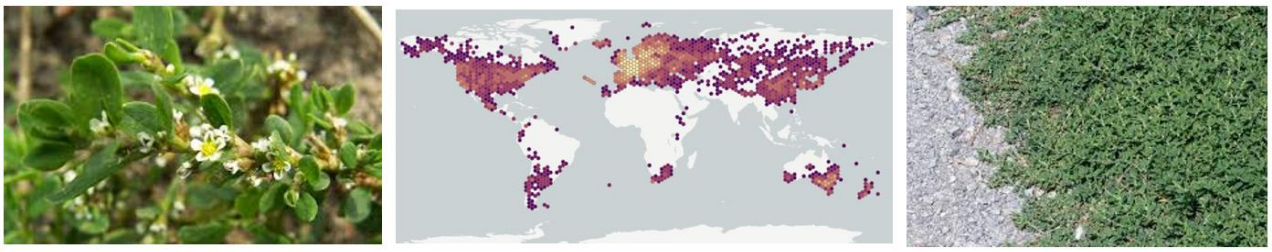


Figure 1 Botanical features and regional distribution of *Polygonum aviculare* L. The figure shows the taxonomic classification, representative plant morphology, and global distribution pattern of *P. aviculare.* These visual data provide an overview of the plant's botanical identity and its wide geographical occurrence.

Kingdom: Plantae
Clade: Tracheophyta
Clade: Angiosperms
Clade: Eudicots
Clade: Asterids
Order: Solanales
Family: Solanaceae
Genus: *Capsicum*
Species: *Capsicum annuum* L.

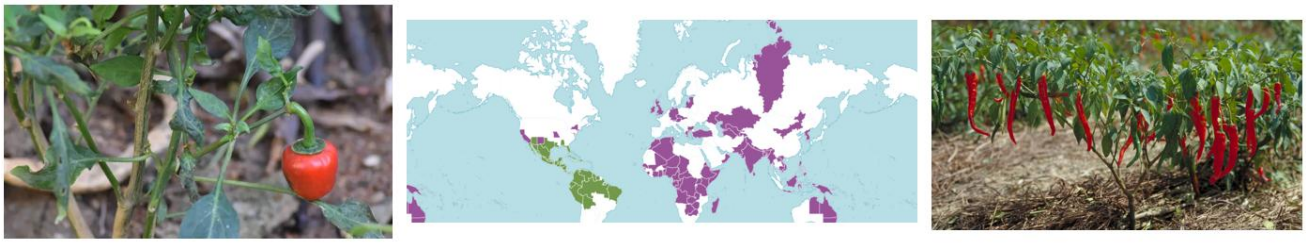


Figure 2 Botanical characteristics and geographical distribution of *Capsicum annuum* L. This figure summarizes the taxonomic position of C. annuum and illustrates its main morphological features, including vegetative growth, fruit development, and mature pepper fruits. The distribution map highlights the wide regional occurrence of the species, indicating its global cultivation, ecological adaptability, and economic importance.

The precipitation of proteins and peptides from the aqueous plant extract was carried out in centrifuge tubes. For this purpose, 1 mL of the investigated sample was mixed with an equal volume (1 mL, exact volume) of 20% trichloroacetic acid (TCA) [9]. After 10 min, the precipitated proteins were separated by centrifugation at 8,000 rpm for 15 min. From the obtained supernatant, 0.1 mL was collected and lyophilized. The dried residue was then evaporated and dissolved in a mixture of triethylamine–acetonitrile–water (1:7:1), followed by drying. This procedure was repeated twice to neutralize residual acidity. Free amino acids were derivatized by reaction with phenyl isothiocyanate (PITC) to obtain phenylthiocarbamyl (PTC) amino acid derivatives according to the method described by Steven A. and Cohen Daviel. Identification of the amino acid derivatives was performed using high-performance liquid chromatography (HPLC). The analytical conditions were as follows: Agilent Technologies 1,200 chromatograph equipped with a DAD detector and a Discovery HS C18 column (75×4.6 mm^2). Mobile phase A consisted of 0.14 M sodium acetate (CH_3COONa) containing 0.05% triethylamine (TEA), pH 6.4, while mobile phase B was acetonitrile (CH_3CN). The flow rate was 1.2 mL/min, and detection was carried out at 269 nm. The gradient program for solvent B was as follows: 1% - 6% (0 - 2.5 min); 6% - 30% (2.51 - 40 min); 30% - 60% (40.1 - 45 min); 60% - 60% (45.1 - 50 min); and 60% - 0% (50.1 - 55 min) [10].

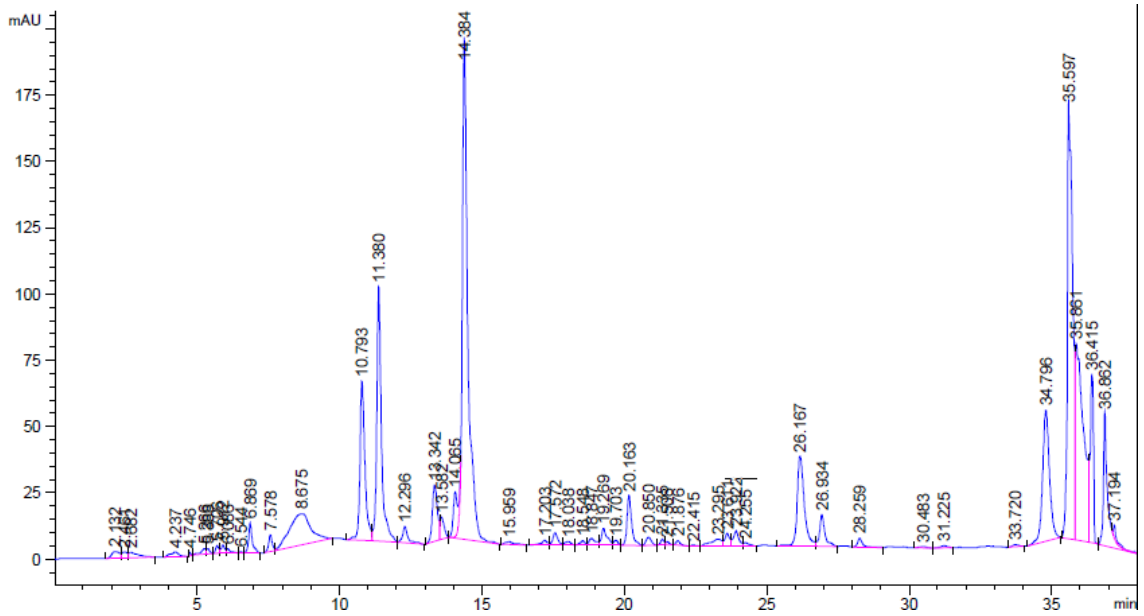


Figure 3 HPLC chromatographic profile of free amino acids detected in AS-Capsipol. This figure illustrates the chromatographic separation of PITC-derived free amino acids in the AS-Capsipol sample using reversed-phase HPLC with DAD detection. The retention-time peaks indicate the presence of multiple amino acid components and support the chemical characterization of AS-Capsipol.

Table 1 Concentration of amino acids identified in the As-Capsipol complex (mg/g).

Amino acids	**As-Capsipol**
	Concentration (mg/g)
Aspartic acid	3.985
Glutamic acid	1.237
Serine	7.551
Glycine	8.767
Asparagine	8.779
Glutamine	10.598
Cysteine	1.398
Threonine	3.763
Arginine	0.458
Alanine	3.080
Proline	64.028
Tyrosine	1.115
Valine	3.404
Methionine	0.895
Histidine	4.874
Isoleucine	1.034
Leucine	1.551
Tryptophan	7.147
Phenylalanine	2.037
Lysine	0.371
Total	**136.071**

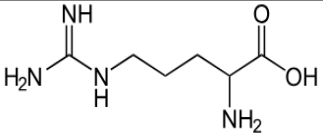
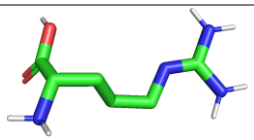
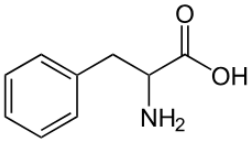
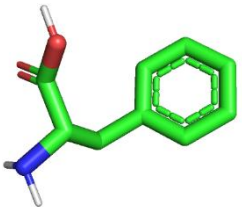
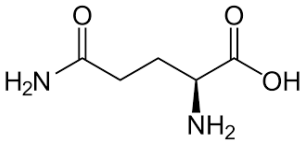
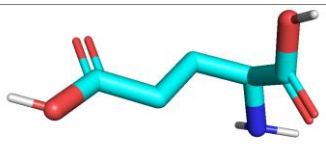
Animal ethics

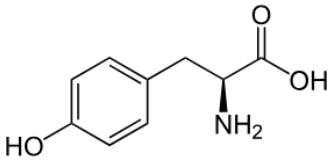
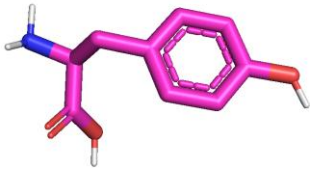
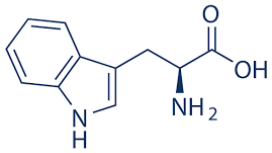
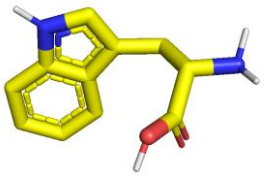
All preoperative and experimental protocols were reviewed and formally approved by the Institutional Animal Care and Use Committee. The animals were housed under standardized vivarium conditions, with controlled environmental parameters including a relative humidity of 55% - 65% and a temperature maintained at 22 ± 2 °C. Throughout the experimental period, the animals had ad libitum access to water and were fed a standard laboratory diet. All experimental procedures and animal handling practices were carried out in strict compliance with the European Directive 2010/63/EU, which governs the ethical use of animals in scientific research and ensures adherence to internationally accepted standards of animal welfare.

Molecular docking: Software and databases

All computational analyses were conducted using freely available academic software tools. The 3-dimensional structures of the selected target proteins, including cyclooxygenase-2 (COX-2, PDB ID: 5IKR), interleukin-6 (IL-6, PDB ID: 1ALU), mitogen-activated protein kinase (MAPK, PDB ID: 1A9U), nuclear factor kappa B (NF-kB, PDB ID: 1NFI), and tumor necrosis factor alpha (TNF-α, PDB ID: 2AZ5), were retrieved from the Protein Data Bank (PDB) [11]. Ligand structures representing amino acids from the As-Capsipol complex were obtained from the PubChem database, where their 3-dimensional conformations were downloaded in suitable formats and subsequently subjected to geometry optimization prior to docking (**Table 2**). Protein preparation and structural inspection were performed using PyMOL (version 1.2) [12]. The active binding sites of the proteins were identified using Discovery Studio, enabling precise localization of docking regions. Visualization and analysis of ligand–protein interactions were also carried out using PyMOL. Molecular docking simulations were conducted using AutoDock 4.2, with AutoDock Tools (ADT) employed for protein and ligand preparation, including the addition of polar hydrogens, assignment of partial charges, and definition of rotatable bonds. Grid box parameters were defined based on the predicted active sites [13]. This methodology allows reliable prediction of ligand binding modes and interaction profiles within the target proteins.

Table 2 Structural representation of selected amino acid ligands in 2D and 3D formats used for molecular docking analysis.

Ligands	2D	3D
Arginine		
Phenylalanine		
Glutamic acid		

Ligands	2D	3D
Tyrosine		
Tryptophan		

Preparation of ligand and protein files

Prior to molecular docking, all retrieved PDB structures were subjected to a comprehensive preprocessing procedure, as native files obtained from the Protein Data Bank are not directly suitable for docking analysis [14]. These structures often contain crystallographic water molecules, co-crystallized ligands, ions, and other heteroatoms that may interfere with docking accuracy. Each protein structure was imported into AutoDock Tools (ADT) for preparation. Crystallographic water molecules and all non-essential heteroatoms were removed to eliminate unwanted interactions. Co-crystallized ligands were deleted before docking simulations; however, they were preserved separately when necessary for validation purposes [15]. Additionally, all non-protein components, including metal ions such as calcium, were excluded to avoid introducing artificial electrostatic effects under the rigid receptor docking model, thereby ensuring uniform treatment of all target proteins. The integrity of each protein structure was visually examined using PyMOL to verify the absence of missing residues in functionally important regions. No critical residues were found to be missing in the selected models [16]. Subsequently, polar hydrogen atoms were added, and Kollman united atom charges were assigned to accurately represent electrostatic properties. Protonation states were adjusted to approximate physiological conditions (pH 7.4) following standard ADT protocols. The prepared receptor structures were then saved in .pdbqt format, which includes atom types and partial charge information required for docking calculations. Ligand preparation was performed in a similar manner. The selected amino acid ligands were imported into ADT, and hydrogen atoms were added, followed by assignment of Gasteiger partial charges. Nonpolar hydrogens were merged in accordance with standard AutoDock procedures [17]. Rotatable bonds and root atoms were automatically defined by the software to allow conformational flexibility during docking. Finally, the ligands were saved in .pdbqt format, containing all necessary structural and electrostatic information for subsequent docking simulations [18].

Calculation of inhibition constant (Ki) from binding energy

In molecular docking studies, the affinity between a ligand and its target protein is typically expressed in terms of binding free energy (ΔG), measured in kcal/mol. Lower (more negative) ΔG values indicate stronger and more favorable interactions. The inhibition constant (Ki), which reflects the binding potency of the ligand, can be estimated from the calculated binding energy using a standard thermodynamic relationship [19].

$$Ki = e\text{^}\frac{\Delta G \times 1000}{R \times T}$$

where, Ki is the inhibition constant (in mol/L); ΔG is the binding free energy (in kcal/mol); R is the universal gas constant = 1.987 cal/(mol·K); T is the temperature in Kelvin (usually 298.15 K); The factor 1,000 converts kcal to cal.

Results and discussion

Acute toxicity of As-Capsipol

The acute toxicity of the As-Capsipol complex obtained from *Polygonum aviculare* L. and *Capsicum*

annuum L. was evaluated in male white outbred mice following a single oral administration at a dose of 2,000 mg/kg. After approximately 8 min of administration, short-term physiological and behavioral changes were observed, including increased respiratory rate, clustering behavior, and narrowing of the eyes. These signs lasted for about 15 - 20 min, after which the animals gradually returned to their normal condition. During the entire 14-day observation period, no mortality was recorded in the As-Capsipol-treated group, and the survival rate remained 100% (5/0). Body weight also remained stable throughout the study. On day 1, the mean body weight of treated animals was 21.1 ± 2.0 g, increasing to 22.1 ± 2.1 g on day 7 and 23.0 ± 2.0 g on day 14. These values did not differ significantly from those of the control group ($p > 0.05$), indicating that the tested dose did not cause a negative effect on body weight gain. No persistent signs of toxicity, severe behavioral abnormalities, convulsions, loss of locomotor activity, or visible deterioration of skin and fur condition were observed. Based on the absence of mortality at 2,000 mg/kg, the median lethal dose (LD50) of As-Capsipol was estimated to be greater than 2,000 mg/kg under the experimental conditions. These findings indicate that As-Capsipol demonstrates low acute toxicity in mice according to the tested dose range. The results are presented in **Table 1**.

Table 3 Assessment of the acute toxicity of the As-Capsipol substance obtained from *Polygonum aviculare* L. and *Capsicum annuum* L. in male mice (M ± m, n = 5).

Groups	Dose (mg/kg, mL)	Number of animals (used/died)	Body weight (g)			LD_{50} (mg/kg)
			Day 1	Day 7	Day 14	
Control (healthy)	(0.4 mL distilled water)	5/0	21.3 ± 2.1	22.2 ± 2.2	23.1 ± 2.3	
As-Capsipol	2,000 mg/kg	5/0	21.1 ± 2.0	22.1 ± 2.1	23.0 ± 2.0	$LD_{50} > 2,000$

The effect of the As-Capsipol substance on the functional parameters of the rat liver

It is well established that acute hepatitis induced by the hepatotoxic drug paracetamol represents a widely accepted experimental model characterized by hepatocyte death. Administration of paracetamol at toxic doses causes intracellular disturbances primarily associated with glutathione (GSH) depletion and accumulation of the toxic metabolite N-acetyl-p-benzoquinone imine (NAPQI) [21]. During the metabolic phase (0 - 3 h), NAPQI binds to cellular proteins, including mitochondrial proteins, thereby initiating early hepatocellular injury (2 - 6 h), which subsequently progresses to apoptosis and necrosis. Given the pathophysiological changes occurring in the liver during acute toxic injury and the possible progression of inflammation to chronic conditions, modern hepatoprotective agents are expected not only to possess antioxidant properties but also to support restoration of liver function and reduce the risk of severe complications such as fibrosis and malignant transformation. In this context, biologically active compounds with multifunctional properties are of considerable interest. In the present study, As-Capsipol was administered at a dose of 150 mg/kg. Hyperenzymemia, reflected by increased alanine aminotransferase (ALT) and aspartate aminotransferase (AST) activities, is a recognized marker of hepatocyte membrane damage and leakage of intracellular enzymes into the bloodstream. As shown in **Table 3**, administration of toxic doses of paracetamol caused marked hepatocellular injury, as evidenced by a statistically significant increase in ALT activity from 58.9 ± 4.7 in healthy animals to 76.8 ± 7.8 in the control group ($p < 0.05$). AST activity was also significantly elevated, increasing from 42.6 ± 4.1 to 61.4 ± 5.9 ($p < 0.05$), further confirming impairment of liver function. Treatment with As-Capsipol at a dose of 150 mg/kg, as well as with the reference drug Heptral, promoted normalization of the studied biochemical parameters. In particular, both treatments reduced transaminase activity and improved urea levels compared with the

control group ($p < 0.05$). These findings indicate that As-Capsipol exerts a hepatoprotective effect under conditions of paracetamol-induced liver injury.

Table 4 Hepatoprotective activity of the As-Capsipol substance in a paracetamol-induced hepatitis model in rats (M ± m, n = 5).

Groups	Dose	Total protein (g/L)	ALT	AST	Urea (mmol/L)
Healthy animals	—	68.6 ± 6.6	58.9 ± 4.7	42.6 ± 4.1	7.4 ± 0.7
Control (water)	—	52.3 ± 1.4*	76.8 ± 7.8*	61.4 ± 5.9*	3.2 ± 0.4*
Geptral	225 mg/kg	66.5 ± 6.2*	55.1 ± 5.3	39.5 ± 4.9*	6.3 ± 0.6*
As-Capsipol	150 mg/kg	63.0 ± 5.6*	52.9 ± 4.8*	38.2 ± 3.3*	5.9 ± 0.5*

Note: * – $p < 0.05$ compared to healthy animals; # – $p < 0.05$ compared to the control group; + – $p < 0.05$ compared to Geptral.

Administration of the reference drug Geptral at a dose of 225 mg/kg and the As-Capsipol substance at a dose of 150 mg/kg for 14 days resulted in a statistically significant reduction of ALT activity in the blood to near physiological levels in rats. The values reached 55.1 ± 5.3 ($p < 0.05$) and 52.9 ± 4.8 ($p < 0.05$), respectively, indicating restoration of hepatocyte integrity and reduced liver damage. Urea, one of the final products of protein and nitrogen metabolism, is synthesized in the liver and excreted through the kidneys. Since this excretion process is continuous, a certain level of urea is normally present in the blood. A decrease in urea concentration is commonly observed in various liver diseases and reflects impaired hepatic synthesis. The results demonstrated that under paracetamol-induced acute hepatitis conditions, the blood urea level decreased almost twofold compared to the physiological norm, from 7.4 ± 0.7 to 3.2 ± 0.4 mmol/L ($p < 0.05$), indicating significant disruption of liver function. At the next stage of the study, renal function was evaluated under conditions of water loading (5% of body weight). Parameters assessed included 4-hour diuresis, serum urea levels (mmol/L), urine pH, and the presence of nitrites, glucose, leukocytes, and other indicators using qualitative reactions with the Combina (Germany) diagnostic kit, as well as microscopic analysis of urinary sediment. The functional state of the kidneys is presented in **Table 2**. After 14 days, renal function was assessed based on diuresis (expressed as the percentage of excreted urine volume relative to the administered fluid over 4 h), urine acidity, and urinary sediment characteristics.

Table 5 Effect of the As-Capsipol substance on selected renal function parameters in a paracetamol-induced hepatitis model in rats (M ± m, n = 5).

Parametrs	Healthy animals	Control	Geptral	As-Capsipol
Urobilinogen	N	N	N	N
Glucose	Neg	Neg	Neg	Neg
Bilirubin	Neg	Neg	Neg	Neg
Ketones	Neg	Neg	Neg	Neg
Specific gravity	1.0125	1.008	1.0175	1.0125
Blood	Neg	Neg	Neg	Neg
pH	7	7	7	7
Protein	Neg	Neg	Neg	Neg
Nitrites	Neg	Neg	Neg	Neg
Leukocytes	Neg	Neg	Neg	Neg

The urea level in the blood serum of rats in the experimental groups differed significantly from that of the control group. In the control group, urea concentration was markedly reduced compared to healthy animals, indicating impaired liver function. In contrast, treatment with As-Capsipol and the reference drug Heptral led to an increase in urea levels toward physiological values, suggesting partial restoration of hepatic metabolic activity. During the study, glucose, protein, and other parameters were not detected in the urine of rats in both experimental and control groups. The urine pH ranged between 7.0 and 7.2. No pathological changes were observed in the urinary sediment.

Pharmacokinetic prediction (BOILED-egg analysis)

The pharmacokinetic properties of the selected amino acids from the As-Capsipol complex were evaluated using the BOILED-Egg model to predict gastrointestinal absorption and blood-brain barrier (BBB) permeability (**Figure 4**). The analysis showed that all investigated amino acids, including arginine, phenylalanine, glutamic acid, tyrosine, and tryptophan, are positioned outside the optimal regions associated with both high gastrointestinal absorption (white region) and BBB permeability (yellow region). This distribution indicates that the analyzed compounds are characterized by limited passive intestinal absorption and a low probability of penetration across the blood-brain barrier under the predicted conditions. Notably, despite minor variations in their positions within the plot, all compounds exhibited a similar pharmacokinetic profile, suggesting consistent physicochemical behavior among the selected amino acids. The observed low BBB permeability may be considered advantageous, as it implies reduced central nervous system exposure and a lower likelihood of CNS-related side effects. At the same time, the predicted limited gastrointestinal absorption highlights potential constraints in oral bioavailability, which may be related to the relatively high polarity and physicochemical properties of these amino acids.

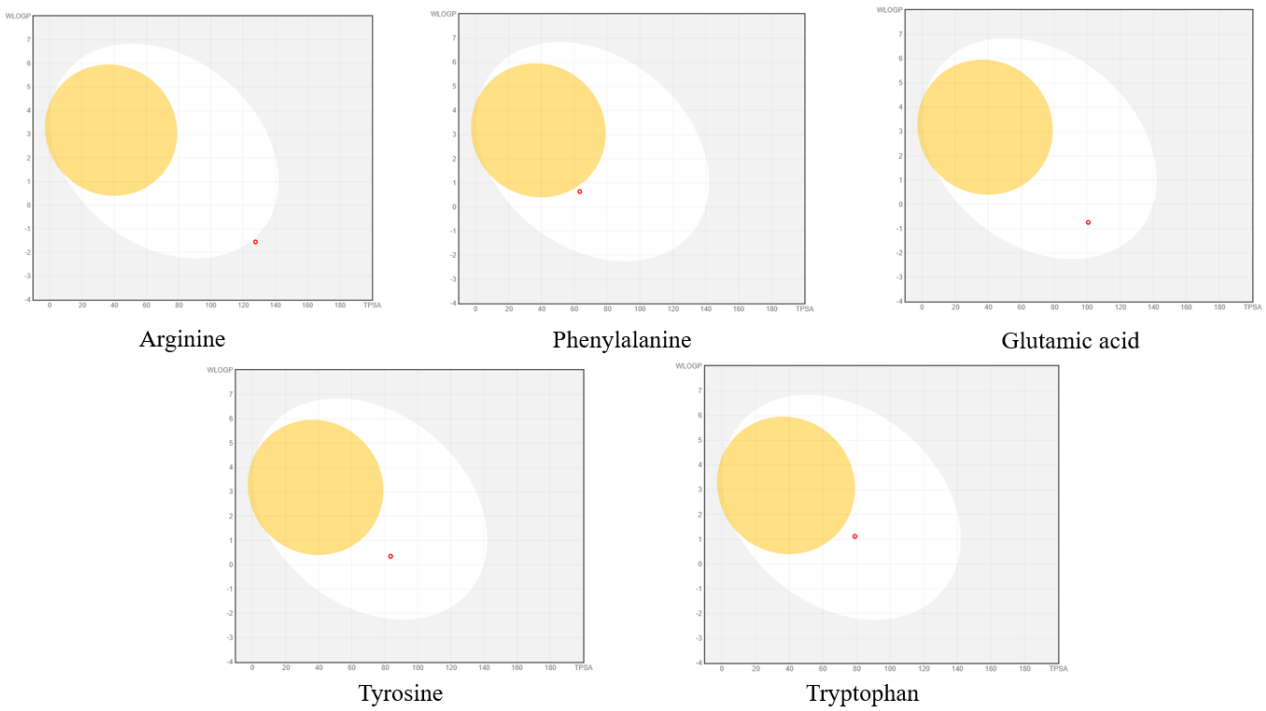


Figure 4 BOILED-Egg model predicting gastrointestinal absorption and blood–brain barrier permeability of selected amino acids from the As-Capsipol complex.

These findings provide supportive *in silico* evidence complementing the experimental results and contribute to a better understanding of the pharmacokinetic characteristics of the As-Capsipol complex components.

Computational tools and databases applied in molecular docking analysis

To elucidate the potential molecular mechanisms underlying the biological activity of the As-Capsipol complex, an *in silico* molecular docking study was performed. The As-Capsipol complex consists of a diverse pool of amino acids; however, for targeted docking analysis, a subset of amino acids, namely arginine, phenylalanine, glutamic acid, tyrosine, and tryptophan, was selected based on their binding affinity profiles and biological relevance. The selection of these amino acids was guided by their favorable binding energies toward the investigated targets, as observed in preliminary docking results. Among them, tryptophan and tyrosine demonstrated the most pronounced binding affinities across multiple targets, indicating strong interaction potential [22]. Phenylalanine also exhibited consistently high binding energies, suggesting its role in stabilizing ligand–protein interactions through hydrophobic and π–π stacking interactions. Arginine was included due to its ability to form strong electrostatic and hydrogen bond interactions via its positively charged guanidinium group, which facilitates binding to negatively charged residues within protein active sites [23]. Glutamic acid, a negatively charged amino acid, was selected based on its capacity to participate in ionic interactions and its involvement in the regulation of inflammatory signaling pathways. The docking analysis was performed against key protein targets implicated in inflammation and liver injury progression, including cyclooxygenase-2 (COX-2, PDB ID: 5IKR), interleukin-6 (IL-6, PDB ID: 1ALU), mitogen-activated protein kinase (MAPK, PDB ID: 1A9U), nuclear factor kappa B (NF-kB, PDB ID: 1NFI), and tumor necrosis factor-alpha (TNF-α, PDB ID: 2AZ5). These targets were selected due to their central roles in inflammatory signaling pathways and the pathogenesis of liver diseases [24].

COX-2

Cyclooxygenase-2 (COX-2) is an inducible enzyme that plays a crucial role in the conversion of arachidonic acid into prostaglandins, particularly during inflammatory responses. Unlike COX-1, which is constitutively expressed in most tissues and involved in maintaining physiological homeostasis, COX-2 expression is typically low under normal conditions but is significantly upregulated in response to inflammatory stimuli such as cytokines, oxidative stress, and viral infections. In the context of hepatitis, COX-2 has been shown to play an important role in the pathogenesis and progression of liver inflammation [25]. Various forms of hepatitis, including viral hepatitis (such as hepatitis B and C), are associated with increased expression of COX-2 in hepatocytes and non-parenchymal liver cells. This upregulation leads to enhanced production of prostaglandin E2 (PGE2), which contributes to hepatic inflammation by promoting vasodilation, increasing vascular permeability, and modulating immune responses. Furthermore, PGE2 can influence the balance between pro-inflammatory and anti-inflammatory cytokines, thereby affecting the severity and persistence of liver injury [26]. Chronic activation of COX-2 in hepatitis is also linked to the progression of liver diseases, including fibrosis, cirrhosis, and hepatocellular carcinoma. COX-2-derived mediators have been reported to stimulate hepatic stellate cell activation, leading to excessive deposition of extracellular matrix components and the development of fibrosis. In addition, COX-2 may contribute to carcinogenesis by promoting cell proliferation, inhibiting apoptosis, and enhancing angiogenesis within the liver microenvironment. Given its significant involvement in liver inflammation and disease progression, COX-2 represents a potential therapeutic target in hepatitis-related conditions [27]. Selective inhibition of COX-2 has been suggested as a strategy to reduce hepatic inflammation and limit disease progression. However, the therapeutic application of COX-2 inhibitors must be carefully evaluated due to their potential systemic side effects, particularly in long-term use.

Arginine showed a binding affinity of −6.1 kcal/mol against COX-2, corresponding to an estimated Ki value of approximately 3.4×10^{-5} M (about 34 μM), indicating moderate inhibitory potential and stable

interaction within the enzyme's active region. The docking simulation was performed using a grid box centered at center_x = 36.323000, center_y = 26.465000, and center_z = 23.686000, allowing accurate positioning of the ligand within the functional binding pocket of COX-2 (**Figure 5**). According to the docking analysis, arginine formed conventional hydrogen bonds with Gln192, Ser353, Leu352, and Met522 (**Figure 6**), while an unfavorable positive–positive interaction was observed with Arg513. The affinity toward these residues can be attributed to the structural features of arginine, particularly its polar guanidinium group, which readily forms hydrogen bonds with polar amino acids. Gln192 and Ser353 play important roles in stabilizing ligand binding through hydrogen bonding, thereby anchoring the ligand within the active site. Although Leu352 is primarily hydrophobic, it contributes to ligand positioning through close-contact interactions. Met522, located within the hydrophobic channel of COX-2, is known to be involved in substrate accommodation, suggesting that arginine occupies a catalytically relevant region. The unfavorable interaction with Arg513 likely arises from electrostatic repulsion between positively charged groups present in both the ligand and the residue. However, this effect is outweighed by multiple stabilizing hydrogen bonds, resulting in an overall favorable binding energy. From a functional perspective, the positioning of arginine within the active site may partially hinder substrate entry or disrupt the proper alignment required for enzymatic catalysis. Given that COX-2 mediates the conversion of arachidonic acid into pro-inflammatory prostaglandins, such interactions may reduce enzymatic activity and contribute to the attenuation of inflammatory processes, which is particularly relevant in the context of hepatitis where COX-2 expression is elevated [28].

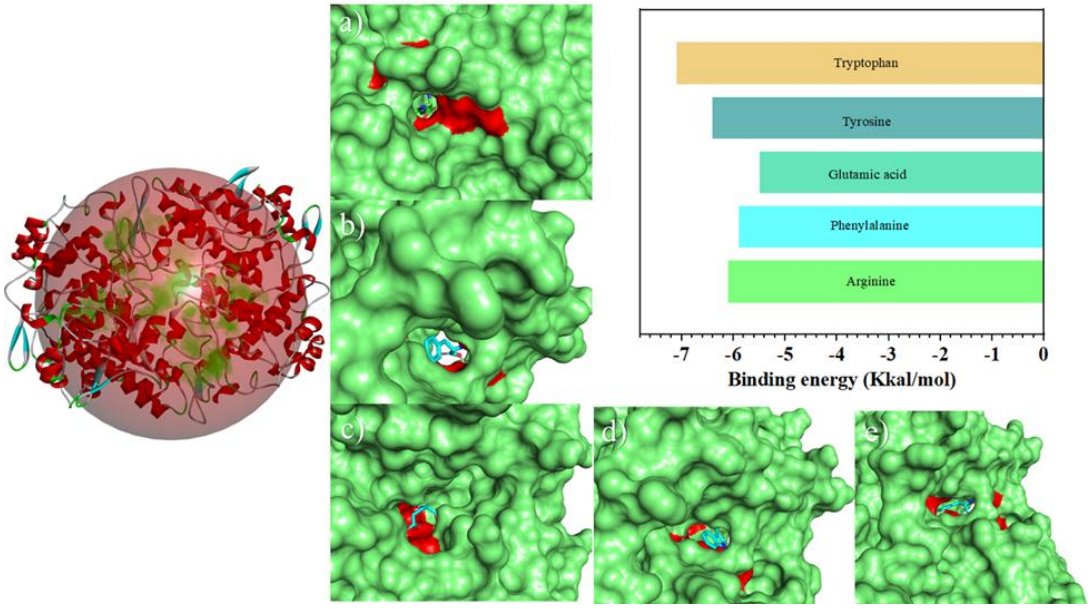


Figure 5 Integrated molecular docking analysis of selected amino acids from the As-Capsipol complex with COX-2, illustrating binding interactions and affinities: (a) arginine, (b) phenylalanine, (c) glutamic acid, (d) tyrosine, and (e) tryptophan.

Phenylalanine demonstrated a binding affinity of −5.9 kcal/mol toward COX-2 (**Figure 5**), which corresponds to an estimated Ki value of approximately 5.2×10^{-5} M, or about 52 μM. This value indicates a moderate inhibitory potential, slightly weaker than that observed for arginine, but still suggesting a meaningful interaction with the enzyme. The interaction analysis shows that phenylalanine forms conventional hydrogen bonds with Cys36, Cys41, and Gln461, indicating stable anchoring within the binding pocket. These residues are polar or semi-polar in nature and are capable of stabilizing the ligand through hydrogen bonding interactions. In particular, cysteine residues such as Cys36 and Cys41 can participate in hydrogen bonding

via their thiol groups, contributing to ligand positioning and stabilization. Gln461, being a polar residue, further enhances binding specificity through hydrogen bond formation. In addition to hydrogen bonding, phenylalanine exhibits π-related interactions due to its aromatic benzene ring. A π–sigma interaction is observed with Leu152, while a π–alkyl interaction occurs with Arg469. These interactions are important because aromatic residues like phenylalanine are well known for their ability to engage in hydrophobic and π-mediated contacts, which significantly contribute to ligand stability within hydrophobic regions of proteins. Such interactions help maintain the ligand in a favorable orientation inside the binding pocket. An unfavorable donor–donor interaction is observed with His39 (**Figure 6**). This can be explained by the presence of competing hydrogen bond donor groups between phenylalanine and the histidine residue, leading to a repulsive interaction. However, similar to the arginine case, this unfavorable contact does not dominate the overall binding, as it is compensated by multiple stabilizing interactions. From a structural and functional perspective, the binding of phenylalanine appears to be driven largely by hydrophobic and aromatic interactions rather than strong electrostatic forces. This suggests that phenylalanine occupies a relatively hydrophobic region of the COX-2 binding site, potentially interfering with substrate accommodation or stabilizing an inactive conformation of the enzyme. Since COX-2 activity depends on proper positioning of arachidonic acid within its hydrophobic channel, the presence of phenylalanine in this region may disrupt substrate binding and reduce enzymatic activity.

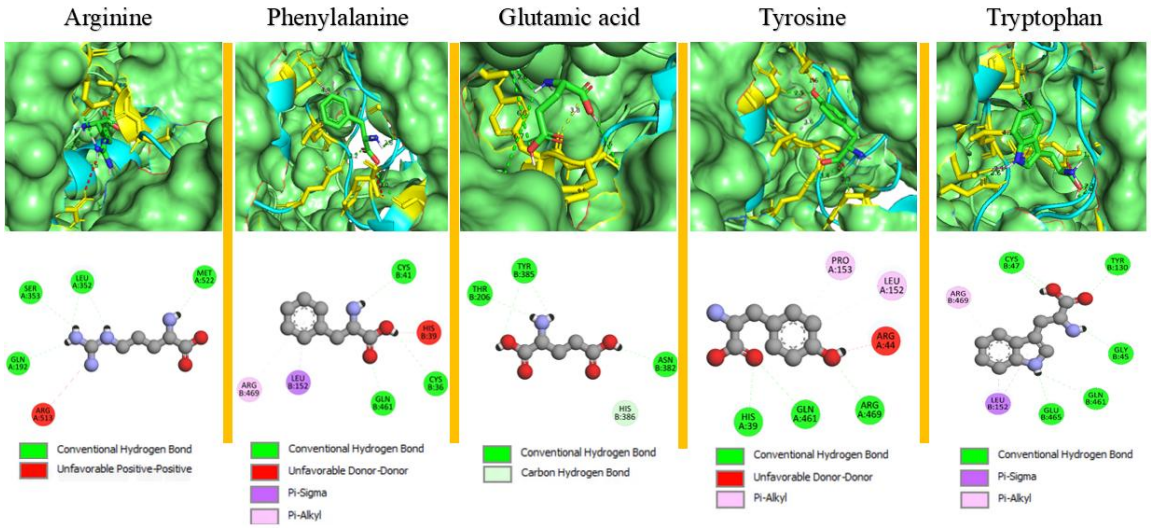


Figure 5 Comprehensive molecular docking visualization of selected As-Capsipol amino acids within the COX-2 active site, illustrating binding modes, interaction networks, and structural alignment for arginine, phenylalanine, glutamic acid, tyrosine, and tryptophan.

Glutamic acid showed a binding affinity of −5.5 kcal/mol toward COX-2 (**Figure 5**), with a corresponding Ki value of approximately 9.3×10^{-5} M (around 93 μM), indicating a moderate level of inhibitory activity. The docking simulation was performed using the grid box centered at coordinates center_x = 36.323000, center_y = 26.465000, and center_z = 23.686000, ensuring proper localization of the ligand within the active site region of the enzyme. Analysis of the interaction pattern revealed that glutamic acid is stabilized within the binding pocket through several hydrogen bonds involving Thr206, Tyr385, and Asn382, along with an additional carbon hydrogen interaction with His386. These amino acid residues are positioned within the functional region of COX-2 and are known to contribute to ligand accommodation and enzymatic activity. In particular, Tyr385 plays a key role in the catalytic mechanism of COX-2 (**Figure 6**), and its involvement in ligand interaction suggests that glutamic acid may influence the enzyme's functional behavior.

Tyrosine exhibited a binding affinity of −6.4 kcal/mol toward COX-2, with an estimated Ki value of approximately 2.0×10^{-5} M (about 20 μM), indicating a relatively strong inhibitory potential compared to other amino acids present in the As-Capsipol complex. The docking simulation was carried out using a grid box centered at coordinates center_x = 36.323000, center_y = 26.465000, and center_z = 23.686000, which allowed proper localization of the ligand within the active site of the enzyme (**Figure 5**). The interaction analysis revealed that tyrosine forms conventional hydrogen bonds with His39, Gln461, and Arg469, contributing to stable anchoring within the binding pocket. In addition, hydrophobic π-alkyl interactions were observed with Pro153 and Leu152, indicating that the aromatic ring of tyrosine is well accommodated within a hydrophobic region of the active site. An unfavorable donor–donor interaction was also detected with Arg44, likely due to repulsion between hydrogen bond donor groups; however, this interaction does not significantly affect the overall stability of the complex. The combination of hydrogen bonding and hydrophobic interactions suggests that tyrosine is effectively stabilized within the functional region of COX-2. His39 and Gln461 play important roles in ligand anchoring, while Arg469 further contributes to ligand positioning (**Figure 6**). The involvement of Pro153 and Leu152 highlights the importance of hydrophobic contacts in maintaining the correct orientation of the ligand within the binding cavity. From a functional perspective, the binding of tyrosine within this region may interfere with substrate access or alter the spatial arrangement of catalytically important residues. Since COX-2 is responsible for the conversion of arachidonic acid into pro-inflammatory prostaglandins, occupation of the active site by tyrosine may reduce enzymatic efficiency. Consequently, this interaction may contribute to the anti-inflammatory potential of the As-Capsipol complex, particularly under conditions associated with increased COX-2 expression, such as hepatitis.

Tryptophan exhibited a binding affinity of −7.1 kcal/mol toward COX-2, with an estimated Ki value of approximately 6.0×10^{-6} M (about 6 μM), indicating a strong inhibitory potential compared to the other amino acids identified in the As-Capsipol complex. The docking analysis was performed using a grid box centered at coordinates center_x = 36.323000, center_y = 26.465000, and center_z = 23.686000, ensuring accurate positioning of the ligand within the active site of the enzyme (**Figure 5**). The interaction profile shows that tryptophan is stabilized within the COX-2 binding pocket through multiple conventional hydrogen bonds involving Cys47, Tyr130, Gly45, Gln461, and Glu465 (**Figure 5**). These residues contribute to ligand anchoring and proper orientation within the active site. In addition to hydrogen bonding, π-related interactions were observed, including π–sigma and π–alkyl contacts with Leu152 and Arg469, highlighting the importance of the aromatic indole ring of tryptophan in stabilizing the ligand within a hydrophobic microenvironment. The presence of both polar and hydrophobic interactions suggests that tryptophan is well accommodated within the functional region of COX-2. Residues such as Gln461 and Glu465 contribute to hydrogen bond stabilization, while Tyr130 and Cys47 further enhance ligand binding through polar contacts. The aromatic structure of tryptophan enables strong interactions with hydrophobic residues, which likely contributes to its relatively high binding affinity. From a functional perspective, the positioning of tryptophan within the active site may significantly interfere with substrate access or disrupt the catalytic environment required for prostaglandin synthesis. Since COX-2 is a key enzyme involved in the production of pro-inflammatory mediators, strong binding of tryptophan may lead to a reduction in enzymatic activity. These findings suggest that tryptophan could play a major role in the anti-inflammatory effect of the As-Capsipol complex, particularly in conditions such as hepatitis where COX-2 is highly expressed.

IL-6

Interleukin-6 (IL-6) is a multifunctional cytokine that plays a central role in the regulation of immune responses, inflammation, and hematopoiesis [29]. It is produced by a wide range of cell types, including macrophages, T cells, endothelial cells, and hepatocytes, particularly in response to infection, tissue injury, and inflammatory stimuli. Under normal physiological conditions, IL-6 contributes to host defense mechanisms; however, its excessive or prolonged production is strongly associated with pathological inflammation. In the context of liver diseases, including hepatitis, IL-6 is considered a key mediator of

inflammatory signaling. During acute and chronic hepatitis, elevated levels of IL-6 are observed in both serum and liver tissue. IL-6 activates intracellular signaling pathways primarily through binding to its receptor complex (IL-6R and gp130), which leads to activation of downstream cascades such as the JAK/STAT3, MAPK, and NF-kB pathways [30]. These signaling pathways regulate the expression of genes involved in inflammation, cell survival, proliferation, and immune modulation. Although IL-6 plays a protective role in early stages of liver injury by promoting hepatocyte survival and regeneration, its sustained activation contributes to disease progression. Chronic elevation of IL-6 has been linked to fibrosis, cirrhosis, and hepatocellular carcinoma. It enhances the activation of hepatic stellate cells, promotes extracellular matrix deposition, and supports a pro-inflammatory microenvironment within the liver. Due to its dual role in both protective and pathological processes, IL-6 has become an important therapeutic target in inflammatory and hepatic diseases. Modulation of IL-6 signaling may help reduce excessive inflammation while preserving its beneficial effects on tissue repair. In silico studies targeting IL-6 are therefore valuable for identifying potential compounds capable of regulating this pathway. Overall, IL-6 is a critical component of the inflammatory network involved in hepatitis, and targeting its activity may contribute to the development of novel therapeutic strategies aimed at controlling liver inflammation and preventing disease progression [31].

Arginine demonstrated a binding affinity of −5.4 kcal/mol toward IL-6, with an estimated Ki value of approximately 1.1×10^{-4} M (around 110 μM), indicating a moderate inhibitory potential. The docking simulation was performed using a grid box centered at coordinates center_x = −45.351000, center_y = 180.123000, and center_z = 40.952000, ensuring appropriate localization of the ligand within the IL-6 binding region (**Figure 7**). The interaction analysis revealed that arginine is stabilized within the binding site primarily through multiple conventional hydrogen bonds involving residues Lys153, Ala152, Pro157, Glu129, Thr130, Arg154, and Arg128 (**Figure 8**). These residues contribute to ligand anchoring and proper orientation within the binding pocket. The presence of several polar and charged amino acids in this region facilitates strong hydrogen bonding interactions with the guanidinium group of arginine, which is highly favorable for ligand stabilization. An unfavorable donor–donor interaction was also observed, likely due to electrostatic repulsion between hydrogen bond donor groups of arginine and nearby residues. However, this interaction does not significantly affect the overall binding stability, as it is compensated by multiple favorable hydrogen bonds. From a structural perspective, the positively charged nature of arginine enables it to interact efficiently with negatively charged and polar residues such as Glu129, enhancing its binding within the IL-6 interface. The distribution of interactions suggests that arginine occupies a functionally relevant region that may be involved in receptor binding or protein–protein interaction. Functionally, binding of arginine to IL-6 may interfere with its interaction with the IL-6 receptor complex, potentially modulating downstream signaling pathways such as JAK/STAT3. As IL-6 is a key mediator of inflammation, particularly in hepatitis, such interactions may contribute to the attenuation of inflammatory signaling. Although the binding affinity is moderate, arginine may still play a supportive role within the As-Capsipol complex through combined or synergistic effects with other amino acids.

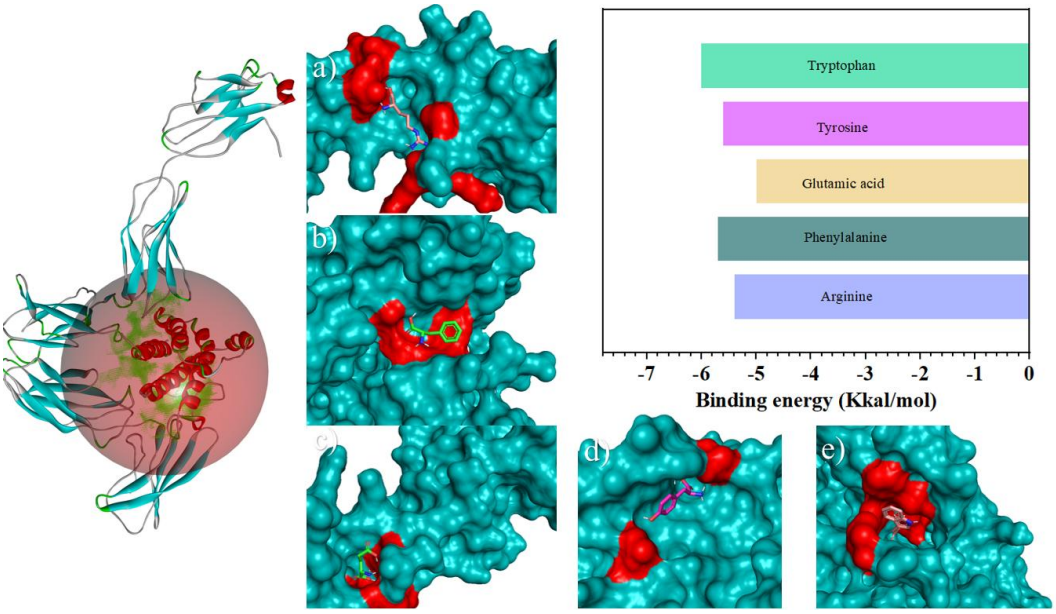


Figure 7 Integrated molecular docking analysis of selected amino acids from the As-Capsipol complex with IL-6, illustrating binding interactions and affinities: (a) arginine, (b) phenylalanine, (c) glutamic acid, (d) tyrosine, and (e) tryptophan.

Phenylalanine exhibited a binding affinity of −5.7 kcal/mol toward IL-6, with an estimated Ki value of approximately 6.6×10^{-5} M (around 66 µM), indicating a moderate inhibitory potential. The docking simulation was performed using a grid box centered at coordinates center_x = −45.351000, center_y = 180.123000, and center_z = 40.952000, which enabled proper localization of the ligand within the selected binding region of IL-6. The interaction pattern revealed that phenylalanine was stabilized through a conventional hydrogen bond with Lys54, a carbon hydrogen bond with Gly193, and a π–π stacked interaction with Phe168. This combination of interactions suggests that the ligand is accommodated within the binding pocket by both polar and aromatic contacts. The hydrogen bond with Lys54 likely contributes to anchoring the ligand, while the interaction with Gly193 may further support local stabilization. Most notably, the π–π stacked interaction with Phe168 reflects favorable aromatic overlap between the benzene ring of phenylalanine and the aromatic side chain of the protein residue, which is a common and energetically important feature in ligand–protein recognition. Structurally, the aromatic character of phenylalanine allows it to interact efficiently with hydrophobic and aromatic regions of the IL-6 binding surface. These contacts may help maintain the ligand in a suitable orientation within the pocket, despite the absence of multiple strong hydrogen bonds. The relatively favorable binding energy suggests that aromatic stabilization plays an important role in the overall ligand affinity. From a functional perspective, binding of phenylalanine within this region may influence the local structural environment of IL-6 and potentially interfere with receptor recognition or protein–protein interactions required for downstream signaling. Since IL-6 is a major pro-inflammatory cytokine involved in the progression of hepatitis and other inflammatory conditions, such interactions may contribute to modulation of IL-6 activity. Thus, phenylalanine may represent one of the amino acid components of the As-Capsipol complex capable of supporting its anti-inflammatory potential.

Glutamic acid exhibited a binding affinity of −5.0 kcal/mol toward IL-6, with an estimated Ki value of approximately 2.2×10^{-4} M (around 220 µM), indicating a moderate but relatively weaker inhibitory potential compared with the other selected amino acids. The docking simulation was carried out using the same grid box centered at center_x = −45.351000, center_y = 180.123000, and center_z = 40.952000, confirming that the ligand was positioned within the selected functional region of IL-6 (**Figure 7**). The interaction analysis showed that glutamic acid formed conventional hydrogen bonds with Gly127, Glu105, and Arg128

(**Figure 8**). In addition, unfavorable donor–donor interactions were observed with Thr130. These findings suggest that glutamic acid is mainly stabilized within the binding pocket through polar contacts, which is consistent with its acidic and highly polar chemical nature. The hydrogen bonds with Gly127 and Arg128 appear to support ligand anchoring, while interaction with Glu105 indicates that glutamic acid is accommodated in a region enriched with polar residues. Because glutamic acid contains negatively charged carboxyl groups, it has a strong tendency to interact with hydrogen-bond-capable residues in the protein environment. However, the presence of unfavorable interactions with Thr130 may reduce the overall stability of the complex, which may explain the slightly weaker binding energy. Despite this, the ligand still maintains a reasonable orientation within the pocket due to the contribution of several stabilizing hydrogen bonds. From a functional point of view, the binding of glutamic acid within this region may influence the local conformation of IL-6 or interfere with amino acid residues involved in receptor recognition. Since IL-6 is an important pro-inflammatory cytokine, even moderate interactions of this kind may contribute to weakening cytokine signaling. Therefore, glutamic acid may still participate in the overall anti-inflammatory potential of the As-Capsipol complex, especially through combined action with other amino acids showing stronger affinity.

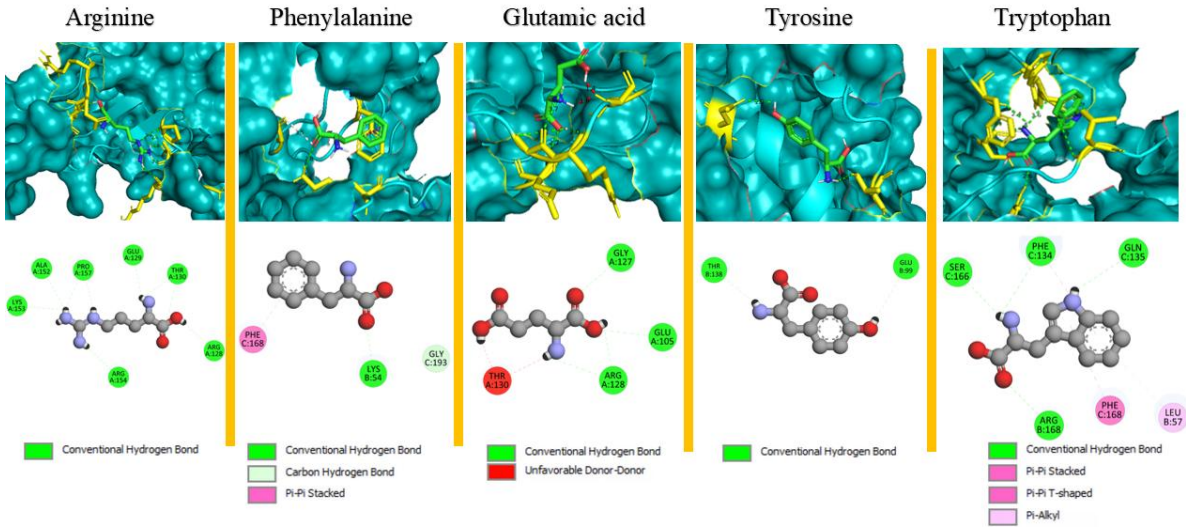


Figure 8 Comprehensive molecular docking visualization of selected As-Capsipol amino acids within the IL-6 active site, illustrating binding modes, interaction networks, and structural alignment for arginine, phenylalanine, glutamic acid, tyrosine, and tryptophan.

Tyrosine exhibited a binding affinity of −5.6 kcal/mol toward IL-6, with an estimated Ki value of approximately 7.9×10^{-5} M (around 79 μM), indicating a moderate inhibitory potential. The docking simulation was performed using a grid box centered at coordinates center_x = −45.351000, center_y = 180.123000, and center_z = 40.952000 (**Figure 7**), confirming that the ligand was positioned within the selected binding region of IL-6. The interaction analysis revealed that tyrosine formed conventional hydrogen bonds with Thr138 and Glu99 (**Figure 8**), which contribute to ligand stabilization within the binding pocket. These residues are capable of forming strong polar interactions, allowing tyrosine to maintain a stable orientation despite a limited number of contacts. The presence of both a hydroxyl group and an aromatic ring in the structure of tyrosine enables it to participate in hydrogen bonding as well as hydrophobic interactions, although in this case the binding appears to be primarily driven by polar contacts. Structurally, the interaction with Thr138 may support ligand anchoring through hydrogen bonding, while Glu99 likely contributes to stabilization via electrostatic and polar interactions. The relatively simple interaction pattern suggests that tyrosine occupies a localized region within the IL-6 structure rather than deeply penetrating the binding interface. This may explain the moderate binding energy observed. From a functional perspective, the binding of

tyrosine to IL-6 may induce minor conformational adjustments or interfere with local residues involved in receptor binding. Although the interaction strength is not as high as that observed for stronger binders, it may still contribute to modulation of IL-6 activity. In the context of the As-Capsipol complex, tyrosine may play a supportive role in regulating inflammatory signaling through combined effects with other amino acids.

Tryptophan exhibited a binding affinity of −6.0 kcal/mol toward IL-6, with an estimated Ki value of approximately 4.0×10^{-5} M (around 40 μM), indicating a moderate to relatively strong inhibitory potential compared to other amino acids in the As-Capsipol complex. The docking simulation was performed using a grid box centered at coordinates center_x = −45.351000, center_y = 180.123000, and center_z = 40.952000 (**Figure 7**), confirming appropriate localization of the ligand within the IL-6 binding region. The interaction analysis revealed that tryptophan formed conventional hydrogen bonds with Ser166, Gln135, and Arg168 (**Figure 8**), contributing to stable ligand anchoring within the binding pocket. In addition, π-related interactions were observed, including π–π stacking with Phe134 and Phe168, as well as π–alkyl interaction with Leu57. These interactions highlight the importance of the aromatic indole ring of tryptophan in stabilizing the ligand within a hydrophobic microenvironment of the protein. Structurally, the presence of both hydrogen bonding and aromatic interactions suggests that tryptophan is well accommodated within the IL-6 binding site. Polar residues such as Gln135 and Ser166 support ligand positioning through hydrogen bonding, while aromatic residues like Phe134 and Phe168 enhance binding stability through π–π interactions. The π–alkyl interaction with Leu57 further contributes to hydrophobic stabilization of the complex. From a functional perspective, the binding of tryptophan to IL-6 may influence the structural conformation of regions involved in receptor recognition or protein–protein interactions. Since IL-6 activity depends on its interaction with receptor complexes, such binding may interfere with signaling processes. Therefore, tryptophan may play a significant role in modulating IL-6-mediated inflammatory pathways, contributing to the overall anti-inflammatory effect of the As-Capsipol complex.

MAPK

Mitogen-activated protein kinases (MAPKs) are a family of serine/threonine kinases that play a central role in transducing extracellular signals into intracellular responses. These kinases are activated by a wide range of stimuli, including cytokines, growth factors, oxidative stress, and inflammatory mediators [32]. The MAPK signaling cascade consists of a 3-tiered phosphorylation pathway involving MAPK kinase kinases (MAP3Ks), MAPK kinases (MAP2Ks), and MAPKs, ultimately leading to the regulation of gene expression. The major MAPK pathways include ERK (extracellular signal-regulated kinase), JNK (c-Jun N-terminal kinase), and p38 MAPK. Among these, the p38 MAPK pathway is particularly important in inflammatory processes and is widely studied in the context of liver diseases, including hepatitis. Activation of MAPK pathways results in the phosphorylation of transcription factors and other regulatory proteins, leading to the expression of pro-inflammatory cytokines such as IL-6 and TNF-α. In hepatic disorders, MAPK signaling is significantly upregulated and contributes to the progression of inflammation, hepatocyte injury, and fibrosis [33]. For instance, activation of p38 MAPK and JNK pathways is associated with increased oxidative stress, mitochondrial dysfunction, and induction of apoptosis in hepatocytes. Moreover, MAPK signaling interacts with other key inflammatory pathways, including NF-kB, amplifying the inflammatory response and promoting chronic liver damage. Due to its central role in regulating inflammation and cell survival, MAPK has emerged as an important therapeutic target. Inhibition of MAPK signaling has been shown to reduce the production of pro-inflammatory mediators, limit hepatocellular damage, and attenuate fibrosis progression. Therefore, compounds capable of modulating MAPK activity are of significant interest in the development of new treatments for inflammatory liver diseases [34]. In silico studies targeting MAPK provide valuable insights into the binding potential of bioactive compounds and their ability to interfere with kinase activity. By identifying molecules that can interact with key residues in the MAPK active site, it is possible to predict their potential as anti-inflammatory and hepatoprotective agents.

Arginine exhibited a binding affinity of −5.3 kcal/mol toward MAPK, with an estimated Ki value of

approximately 1.3×10^{-4} M (around 130 µM), indicating a moderate inhibitory potential. The docking simulation was performed using a grid box centered at coordinates center_x = 3.247000, center_y = 17.679000, and center_z = 31.593000 (**Figure 9**), confirming that the ligand was positioned within the selected functional region of the MAPK binding pocket. The interaction analysis showed that arginine formed conventional hydrogen bonds with Leu75, Lys76, Met78, His80, Val83, and Gly85 (**Figure 10**). In addition, an unfavorable positive–positive interaction was observed with Lys79. This binding pattern suggests that arginine is mainly stabilized through multiple polar contacts, which is consistent with the strongly basic and hydrophilic nature of its guanidinium group. These hydrogen bonds likely help anchor the ligand within the active site and maintain a favorable orientation inside the binding cavity. Leu75 and Val83 may contribute to local stabilization through close-contact interactions, while Lys76, Met78, His80, and Gly85 appear to support ligand accommodation through hydrogen bonding. The unfavorable interaction with Lys79 is most likely caused by electrostatic repulsion between positively charged groups of the ligand and the residue (**Figure 9**). However, this destabilizing effect is compensated by the presence of several favorable hydrogen bonds, allowing the complex to remain overall stable. From a functional perspective, the positioning of arginine within this region may interfere with the catalytic environment of MAPK or affect access of physiological substrates to the active pocket. Since MAPK is a key mediator in intracellular inflammatory signaling pathways, binding of arginine to this site may contribute to downregulation of kinase-associated signaling events. Although the binding strength is moderate, arginine may still participate in the overall biological activity of the As-Capsipol complex through its combined effect with other amino acids showing stronger affinities.

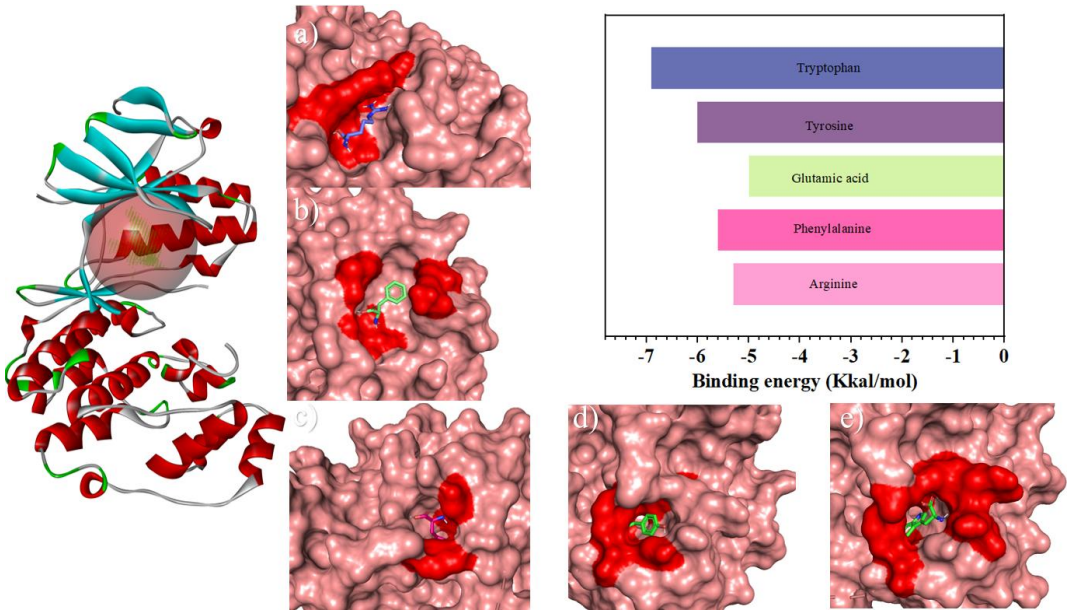


Figure 9 Integrated molecular docking analysis of selected amino acids from the As-Capsipol complex with MAPK, illustrating binding interactions and affinities: (a) arginine, (b) phenylalanine, (c) glutamic acid, (d) tyrosine, and (e) tryptophan.

Phenylalanine demonstrated a binding energy of −5.6 kcal/mol against MAPK, with a corresponding Ki value of approximately 7.9×10^{-5} M (around 79 µM), reflecting a moderate inhibitory effect. The docking procedure was conducted using a grid box centered at center_x = 3.247000, center_y = 17.679000, and center_z = 31.593000, ensuring correct placement of the ligand within the active region of the kinase (**Figure 8**). Analysis of the interaction profile indicates that phenylalanine is stabilized within the binding pocket through several hydrogen bonds involving Asp88, Val89, Ile346, and Phe348 (**Figure 10**). Additionally, a

π–alkyl interaction with Arg5 contributes to hydrophobic stabilization, while an unfavorable acceptor–acceptor interaction is observed with Val345. These results suggest that both polar and hydrophobic interactions are involved in maintaining the ligand within the binding site. The aromatic side chain of phenylalanine appears to be well accommodated within a hydrophobic environment, which supports its proper orientation and contributes to overall binding stability. Residues such as Asp88 and Val89 likely play a role in anchoring the ligand, whereas Ile346 and Phe348 further reinforce the interaction through close contacts within the pocket. Although the interaction with Val345 introduces some destabilization, its effect is relatively minor compared to the stabilizing interactions present. Functionally, the presence of phenylalanine in this region may influence the structural conformation of the MAPK active site or interfere with substrate binding. Given the central role of MAPK in inflammatory signaling pathways, such interactions may contribute to the modulation of kinase activity. Therefore, phenylalanine may act as one of the contributing components of the As-Capsipol complex in regulating MAPK-associated inflammatory responses.

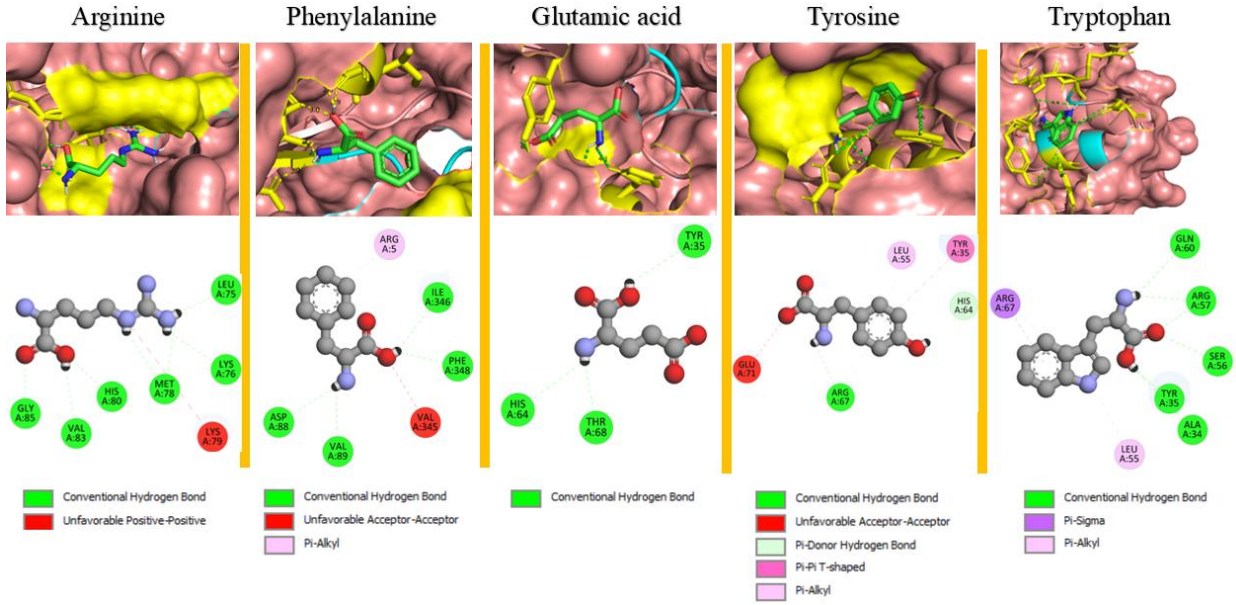


Figure 10 Comprehensive molecular docking visualization of selected As-Capsipol amino acids within the MAPK active site, illustrating binding modes, interaction networks, and structural alignment for arginine, phenylalanine, glutamic acid, tyrosine, and tryptophan.

Glutamic acid showed a binding affinity of −5.0 kcal/mol toward MAPK, with an estimated Ki value of approximately 2.2×10^{-4} M (around 220 μM), indicating a moderate but relatively weaker inhibitory potential. The docking analysis was performed using a grid box centered at coordinates center_x = 3.247000, center_y = 17.679000, and center_z = 31.593000 (**Figure 8**), confirming that the ligand was positioned within the selected region of the MAPK binding pocket (**Figure 8**). The interaction profile revealed that glutamic acid forms conventional hydrogen bonds with Tyr35, His64, and Thr68, which contribute to stabilizing the ligand within the binding site. These residues are capable of forming polar interactions, allowing glutamic acid to maintain a consistent orientation inside the pocket. The presence of multiple carboxyl groups in glutamic acid supports its ability to engage in hydrogen bonding with surrounding amino acids. Structurally, the ligand appears to be accommodated within a polar microenvironment, where residues such as His64 and Thr68 play an important role in anchoring the molecule. Interaction with Tyr35 further enhances stabilization through hydrogen bonding. Although the number of interactions is limited compared to stronger binders, they are sufficient to maintain ligand positioning within the active region (**Figure 10**). From a functional perspective, the binding of glutamic acid within this region may induce minor conformational changes or interfere with residues

involved in substrate binding and catalytic activity. Given the role of MAPK in regulating inflammatory signaling pathways, such interactions may contribute to modulation of kinase activity. Despite its moderate affinity, glutamic acid may still participate in the overall biological effect of the As-Capsipol complex through combined or synergistic interactions with other amino acids.

Tyrosine demonstrated a binding affinity of −6.0 kcal/mol toward MAPK, with an estimated Ki value of approximately 4.0×10^{-5} M (around 40 μM), indicating a moderate to relatively strong inhibitory potential. The docking simulation was performed using a grid box centered at coordinates center_x = 3.247000, center_y = 17.679000, and center_z = 31.593000, confirming appropriate positioning of the ligand within the MAPK binding region (**Figure 9**). The interaction analysis revealed that tyrosine formed a conventional hydrogen bond with Arg67, contributing to ligand anchoring within the binding pocket. Additionally, π-related interactions were observed, including a π–π T-shaped interaction with Tyr35 and a π–alkyl interaction with Leu55, highlighting the role of the aromatic ring of tyrosine in stabilizing the ligand within a hydrophobic environment (**Figure 10**). A π-donor hydrogen bond interaction with His64 was also identified, further supporting ligand accommodation. However, an unfavorable acceptor–acceptor interaction was observed with Glu71, which may introduce a degree of local destabilization. Structurally, the combination of hydrogen bonding and aromatic interactions suggests that tyrosine is well accommodated within the active site of MAPK. The interaction with Arg67 likely supports stable positioning, while aromatic contacts with Tyr35 and Leu55 enhance binding through hydrophobic and π-mediated interactions. The involvement of His64 adds an additional stabilizing component through polar interaction. Although the unfavorable contact with Glu71 may slightly reduce binding strength, it does not negate the overall stability of the complex. From a functional perspective, the binding of tyrosine within this region may influence the conformation of the MAPK active site or interfere with substrate recognition. Given the role of MAPK in regulating inflammatory signaling pathways, such interactions may contribute to modulation of kinase activity. Therefore, tyrosine may play an important role among the amino acid components of the As-Capsipol complex in affecting MAPK-mediated inflammatory responses.

Tryptophan showed a binding energy of −6.9 kcal/mol against MAPK, with an estimated Ki value of approximately 8.7×10^{-6} M (around 8.7 μM), indicating a relatively strong inhibitory capacity among the amino acids present in the As-Capsipol complex. The docking was carried out using a grid box centered at center_x = 3.247000, center_y = 17.679000, and center_z = 31.593000 (**Figure 8**), ensuring correct placement of the ligand within the active region of the kinase. Interaction analysis indicated that tryptophan is stabilized within the binding pocket through several hydrogen bonds involving Gln60, Arg57, Ser56, Tyr35, and Ala34 (**Figure 10**). These interactions help maintain firm anchoring and proper positioning of the ligand. In addition to these polar contacts, aromatic interactions were observed, including a π–sigma interaction with Arg67 and a π–alkyl interaction with Leu55, which further enhance the stability of the complex. The presence of both hydrogen bonding and hydrophobic interactions suggests that tryptophan fits well into the MAPK binding site. Residues such as Gln60, Arg57, and Ser56 contribute to stabilization through polar interactions, while Tyr35 and Ala34 support ligand accommodation within the pocket. The aromatic nature of tryptophan allows it to form additional stabilizing contacts with surrounding residues, improving its overall binding strength. From a functional standpoint, the positioning of tryptophan within this region may disrupt substrate binding or alter the catalytic environment of MAPK. Considering the key role of MAPK in inflammatory signaling pathways, such interactions may contribute to reducing kinase activity. Therefore, tryptophan may play a significant role in the overall biological effect of the As-Capsipol complex, particularly in modulating MAPK-related inflammatory processes.

NF-kB

Nuclear factor kappa B (NF-kB) is a key transcription factor that plays a central role in the regulation of immune responses, inflammation, and cell survival. It is normally present in the cytoplasm in an inactive form, bound to inhibitory proteins known as IkBs [35]. Upon stimulation by various signals such as cytokines, oxidative stress, or pathogens, IkB proteins

are degraded, allowing NF-kB to translocate into the nucleus where it regulates the expression of a wide range of genes. NF-kB controls the transcription of numerous pro-inflammatory mediators, including cytokines such as IL-6 and TNF-α, chemokines, adhesion molecules, and enzymes like COX-2. In the context of liver diseases, particularly hepatitis, NF-kB is highly activated and contributes to the amplification of inflammatory responses. Its activation leads to sustained production of inflammatory cytokines, promoting hepatocyte injury, immune cell infiltration, and progression toward chronic inflammation [36]. In addition to its role in inflammation, NF-kB is also involved in regulating apoptosis and cell proliferation. While transient activation may support cell survival and tissue repair, prolonged or dysregulated NF-kB signaling is associated with pathological conditions such as fibrosis, cirrhosis, and hepatocellular carcinoma. NF-kB signaling is closely interconnected with other pathways, including MAPK and JAK/STAT, creating a complex network that drives disease progression [37]. Due to its central role in controlling inflammatory gene expression, NF-kB has become an important therapeutic target. Inhibition of NF-kB activation can suppress the production of pro-inflammatory mediators and reduce tissue damage. Therefore, compounds capable of interacting with NF-kB or its regulatory components may provide beneficial effects in the treatment of inflammatory liver diseases [38]. In silico docking studies targeting NF-kB help to identify molecules that can bind to key regions involved in DNA binding or protein–protein interactions, thereby potentially blocking its transcriptional activity. Such approaches are valuable for understanding the molecular basis of anti-inflammatory effects and for guiding the development of novel therapeutic agents.

Arginine demonstrated a binding affinity of −5.8 kcal/mol toward NF-kB, with an estimated Ki value of approximately 5.6×10^{-5} M (around 56 μM), indicating a moderate inhibitory potential. The docking simulation was carried out using a grid box centered at center_x = 27.659000, center_y = 19.514000, and center_z = 36.394000 (**Figure 11**), confirming that the ligand was properly positioned within the DNA-binding region of the NF-kB complex. Interaction analysis revealed that arginine formed multiple conventional hydrogen bonds with nucleotide residues, including DG720, DG722, DG717, DA721, and DT716 (**Figure 12**). These interactions suggest that arginine is capable of directly associating with the DNA interface of NF-kB rather than only the protein component. The presence of several hydrogen bonds highlights the strong affinity of arginine's guanidinium group for negatively charged phosphate backbones and polar regions of nucleotides, which facilitates stable binding within the complex. The interaction pattern indicates that arginine is well accommodated within a highly polar environment dominated by nucleic acid residues. Its positively charged structure enables efficient electrostatic attraction and hydrogen bond formation with DNA bases and backbone atoms, contributing to ligand stabilization. Such positioning may interfere with the normal binding of NF-kB to DNA or alter the stability of the transcription factor–DNA complex. From a functional perspective, this type of interaction is particularly important because NF-kB exerts its biological activity through binding to specific DNA sequences and regulating gene transcription. The association of arginine within this region may hinder DNA recognition or disrupt transcriptional activation of pro-inflammatory genes such as IL-6 and TNF-α. Therefore, arginine, as part of the As-Capsipol complex, may contribute to the suppression of NF-kB-mediated inflammatory signaling, which is especially relevant in the context of hepatitis-related inflammation.

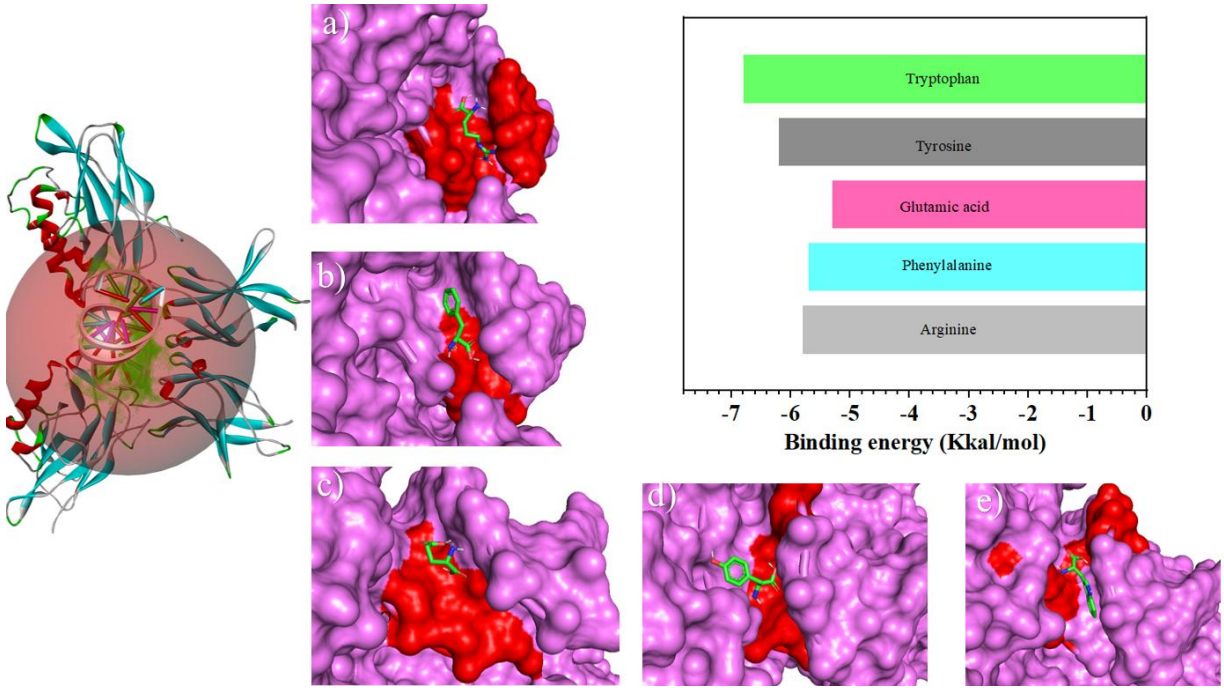


Figure 11 Integrated molecular docking analysis of selected amino acids from the As-Capsipol complex with NF-kB, illustrating binding interactions and affinities: (a) arginine, (b) phenylalanine, (c) glutamic acid, (d) tyrosine, and (e) tryptophan.

Phenylalanine exhibited a binding affinity of −5.7 kcal/mol toward NF-kB, with an estimated Ki value of approximately 6.6×10^{-5} M (around 66 μM), indicating a moderate inhibitory potential. The docking analysis was performed using a grid box centered at coordinates center_x = 27.659000, center_y = 19.514000, and center_z = 36.394000 (**Figure 11**), confirming proper localization of the ligand within the functional binding region of the NF-kB complex. The interaction profile revealed that phenylalanine formed conventional hydrogen bonds with nucleotide residues DA721 and DG720 (**Figure 12**). These results suggest that the ligand interacts directly with the DNA-associated region of the NF-kB complex. Although the number of contacts is limited compared with some other amino acids, the observed hydrogen bonds indicate that phenylalanine is still able to achieve stable accommodation within this binding environment. The aromatic structure of phenylalanine likely contributes to its positioning within the complex by supporting hydrophobic packing and spatial compatibility with the surrounding nucleic acid framework. At the same time, the polar carboxyl and amino groups of the ligand enable hydrogen-bond formation with the nucleotide residues, helping to maintain the ligand in a favorable orientation. This combination of structural features may explain the overall moderate binding energy observed. From a functional perspective, binding of phenylalanine in this region may influence the interaction between NF-kB and DNA, potentially affecting transcriptional activation of inflammation-related genes. Since NF-kB regulates the expression of key pro-inflammatory mediators, even moderate binding at the DNA interface may contribute to reduced signaling activity. Therefore, phenylalanine may participate in the anti-inflammatory effect of the As-Capsipol complex through partial modulation of NF-kB-mediated transcription.

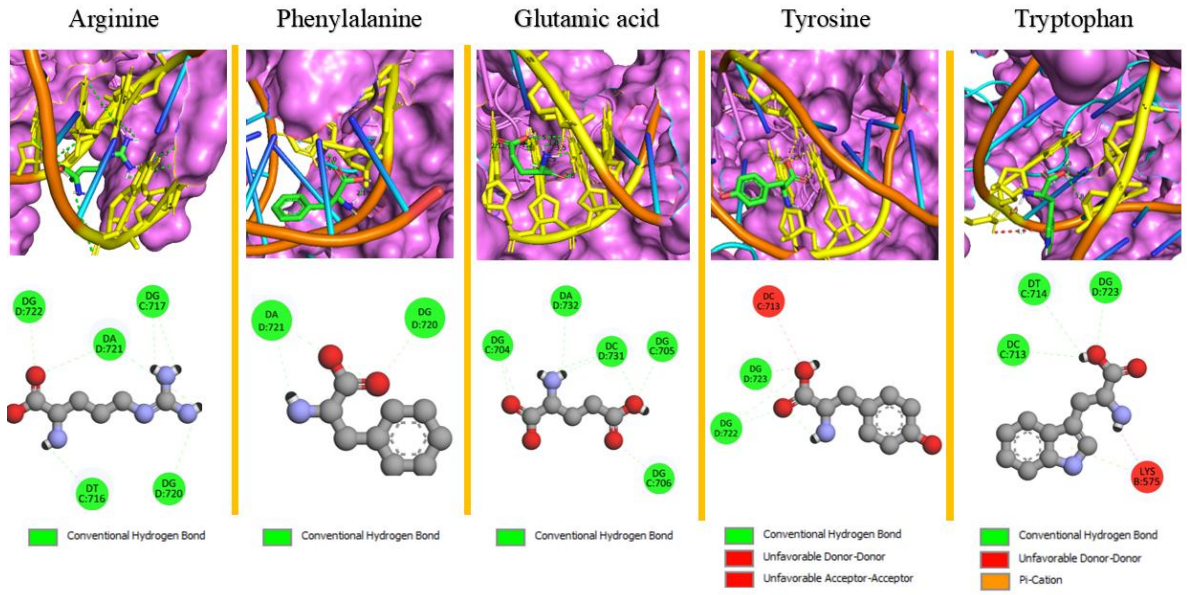


Figure 12 Comprehensive molecular docking visualization of selected As-Capsipol amino acids within the NF-kB active site, illustrating binding modes, interaction networks, and structural alignment for arginine, phenylalanine, glutamic acid, tyrosine, and tryptophan.

Glutamic acid demonstrated a binding affinity of −5.3 kcal/mol toward NF-kB, with an estimated Ki value of approximately 1.3×10^{-4} M (around 130 μM), indicating a moderate inhibitory potential. The docking simulation was performed using a grid box centered at coordinates center_x = 27.659000, center_y = 19.514000, and center_z = 36.394000 (**Figure 11**), confirming that the ligand was localized within the DNA-associated binding region of the NF-kB complex. The interaction analysis revealed that glutamic acid formed multiple conventional hydrogen bonds with nucleotide residues DG704, DA732, DC731, DG705, and DG706 (**Figure 12**). This interaction profile suggests that glutamic acid is capable of establishing stable contacts with the nucleic acid component of the NF-kB complex. Its polar carboxyl and amino groups appear to facilitate these hydrogen-bonding interactions, allowing the ligand to remain favorably positioned within the binding interface. Because glutamic acid contains acidic functional groups, it is well suited for interaction with polar atoms present in nucleotide bases and the DNA backbone. The presence of several hydrogen bonds indicates that the ligand is well accommodated in this highly polar microenvironment. Although the binding energy is moderate, the number of stabilizing contacts suggests that glutamic acid can maintain a meaningful association with the complex. From a functional standpoint, binding of glutamic acid within the DNA-contact region of NF-kB may disturb the normal interaction between the transcription factor and its target DNA sequence. Since NF-kB activity depends on stable DNA binding for transcriptional activation of inflammatory genes, such interactions may contribute to reduced signaling efficiency. Therefore, glutamic acid may participate in the anti-inflammatory action of the As-Capsipol complex by helping to modulate NF-kB-dependent transcriptional responses.

Tyrosine exhibited a binding affinity of −6.2 kcal/mol toward NF-kB, with an estimated Ki value of approximately 2.8×10^{-5} M (around 28 μM), indicating a relatively strong inhibitory potential. The docking simulation was carried out using a grid box centered at coordinates center_x = 27.659000, center_y = 19.514000, and center_z = 36.394000, confirming that the ligand was positioned within the DNA-associated binding region of the NF-kB complex. The interaction profile showed that tyrosine formed conventional hydrogen bonds with DG722 and DG723, which helped stabilize the ligand within the binding interface. At the same time, unfavorable donor–donor and acceptor–acceptor interactions were detected with DC713, suggesting the presence of local steric or electrostatic repulsion. Despite these unfavorable contacts, the overall binding energy remained favorable, indicating

that the stabilizing interactions were sufficient to maintain the complex. The aromatic ring and hydroxyl-containing structure of tyrosine allow it to participate in both polar and spatially favorable interactions within the NF-kB–DNA complex. The hydrogen bonds with DG722 and DG723 suggest that tyrosine interacts directly with nucleotide residues in the DNA-contact region, which may influence the stability of transcription factor binding. Although the unfavorable interaction with DC713 may slightly reduce binding strength, it does not eliminate the ligand's overall affinity for this region. From a functional perspective, the localization of tyrosine within the DNA-binding interface of NF-kB may interfere with the transcription factor's ability to recognize or stably bind its target DNA sequence. Since NF-kB-mediated inflammatory signaling depends on efficient DNA binding and transcriptional activation of downstream genes, such interactions may contribute to suppression of pro-inflammatory gene expression. Therefore, tyrosine may serve as one of the important contributors to the anti-inflammatory potential of the As-Capsipol complex through modulation of NF-kB activity.

Tryptophan demonstrated a binding affinity of −6.8 kcal/mol toward NF-kB, with an estimated Ki value of approximately 1.0×10^{-5} M (around 10 μM), indicating a relatively strong inhibitory potential among the studied amino acids. The docking simulation was performed using a grid box centered at coordinates center_x = 27.659000, center_y = 19.514000, and center_z = 36.394000 (**Figure 11**), confirming proper localization of the ligand within the DNA-binding region of the NF-kB complex. The interaction analysis showed that tryptophan formed multiple conventional hydrogen bonds with nucleotide residues DT714, DG723, and DC713, which contributed to stable ligand anchoring within the binding interface. In addition, a π–cation interaction with Lys575 was observed, highlighting the role of the aromatic indole ring of tryptophan in forming stabilizing electrostatic contacts. However, an unfavorable donor–donor interaction with Lys575 was also detected, suggesting a localized repulsive effect. The combination of hydrogen bonding with nucleotides and π–cation interaction with Lys575 indicates that tryptophan is well accommodated within a mixed nucleic acid–protein environment. The hydrogen bonds help maintain proper positioning of the ligand, while the aromatic system enhances stability through additional non-covalent interactions. Although the unfavorable contact introduces some degree of destabilization, it does not significantly affect the overall binding affinity, as reflected by the relatively low binding energy. From a functional perspective, the localization of tryptophan within the DNA-binding interface of NF-kB may interfere with the transcription factor's interaction with DNA. Since NF-kB activity depends on stable binding to specific DNA sequences to regulate pro-inflammatory gene expression, such interactions may reduce transcriptional efficiency. Therefore, tryptophan may contribute significantly to the anti-inflammatory potential of the As-Capsipol complex by modulating NF-kB-mediated signaling pathways.

TNF-α

Tumor necrosis factor alpha (TNF-α) is a key pro-inflammatory cytokine that plays a central role in the regulation of immune responses, inflammation, and cell death [39]. It is primarily produced by activated macrophages, Kupffer cells in the liver, and other immune cells in response to infection, toxins, or tissue injury. TNF-α acts as an early mediator of inflammation and is involved in initiating and amplifying inflammatory signaling cascades. In the context of liver diseases such as hepatitis, TNF-α is significantly upregulated and contributes to hepatocyte damage. It promotes inflammation by stimulating the production of other cytokines, including IL-6, and activating downstream signaling pathways such as NF-kB and MAPK. Excessive TNF-α activity leads to increased oxidative stress, mitochondrial dysfunction, and induction of apoptosis or necrosis in hepatocytes, thereby aggravating liver injury. TNF-α exerts its biological effects through binding to its receptors, TNFR1 and TNFR2, which trigger multiple intracellular signaling pathways. Activation of these receptors can lead to either cell survival through NF-kB activation or cell death through caspase-mediated apoptosis, depending on the cellular context. This dual role makes TNF-α a critical regulator of inflammation and tissue homeostasis. Due to its pivotal involvement in inflammatory processes, TNF-α is considered an important therapeutic target [40]. Inhibition of TNF-α or disruption of its receptor interactions can reduce

inflammation, prevent hepatocyte damage, and improve liver function. This is particularly relevant in hepatitis, where controlling TNF-α-mediated signaling may limit disease progression and associated complications. *In silico* docking studies targeting TNF-α are useful for identifying molecules that can interfere with cytokine-receptor interactions or destabilize its active conformation. Compounds capable of binding effectively to TNF-α may reduce its biological activity and suppress downstream inflammatory pathways [41]. Therefore, evaluating the interaction of As-Capsipol-derived amino acids with TNF-α provides valuable insight into their potential anti-inflammatory and hepatoprotective mechanisms.

Arginine showed a binding affinity of −6.2 kcal/mol toward TNF-α, with an estimated Ki value of approximately 2.8×10^{-5} M (around 28 μM), indicating relatively strong inhibitory potential. The docking simulation was performed using a grid box centered at center_x = −42.604000, center_y = 96.193000, and center_z = 3.821000 (**Figure 13**), confirming that the ligand was positioned within a functionally relevant region of the TNF-α structure. Interaction analysis revealed that arginine formed conventional hydrogen bonds with Ser60, Gln61, Tyr119, Tyr151, and Leu120. These interactions indicate stable accommodation of the ligand within the binding pocket. The guanidinium group of arginine, which is highly polar and positively charged, appears to play a major role in ligand stabilization through multiple hydrogen-bonding contacts with surrounding residues. The presence of several hydrogen bonds suggests that arginine can maintain a favorable orientation within the target region despite its relatively simple structure. From a structural perspective, the interaction with Ser60 and Gln61 may contribute to initial ligand anchoring, whereas Tyr119 and Tyr151 likely enhance stabilization through additional polar contacts (Figure 14). The hydrogen bond with Leu120 further supports proper positioning of the ligand in the binding site. The overall interaction pattern suggests that arginine is well accommodated in a polar microenvironment of TNF-α. From a functional point of view, binding of arginine in this region may interfere with the conformational stability of TNF-α or affect residues involved in receptor recognition. Since TNF-α is a major pro-inflammatory cytokine, such interactions may weaken downstream inflammatory signaling. Therefore, arginine may contribute to the anti-inflammatory potential of the As-Capsipol complex through modulation of TNF-α activity.

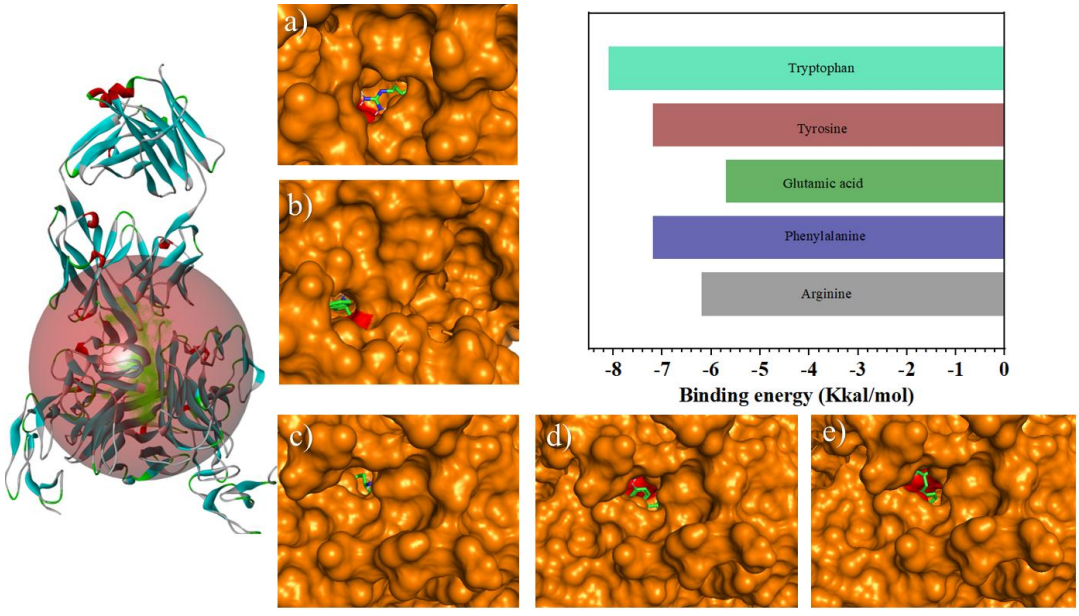


Figure 13 Integrated molecular docking analysis of selected amino acids from the As-Capsipol complex with TNF alpha, illustrating binding interactions and affinities: (a) arginine, (b) phenylalanine, (c) glutamic acid, (d) tyrosine, and (e) tryptophan.

Phenylalanine demonstrated a binding affinity of −7.2 kcal/mol toward TNF-α, corresponding to an estimated Ki value of approximately 5.3×10^{-6} M (about 5.3 μM), which indicates a relatively strong interaction. Docking was performed using a grid box centered at center_x = −42.604000, center_y = 96.193000, and center_z = 3.821000 (**Figure 13**), confirming that the ligand occupied a functionally significant region of the TNF-α protein. The interaction analysis revealed that phenylalanine was primarily stabilized by hydrophobic and aromatic interactions rather than hydrogen bonding. A π–π stacking interaction was observed with Tyr59, while a π–sigma interaction occurred with Leu57, both contributing to the stable positioning of the ligand within the binding pocket. The aromatic ring of phenylalanine plays a key role in these interactions, facilitating favorable contacts within the hydrophobic environment of the protein. An unfavorable acceptor–acceptor interaction with Leu120 was also identified (**Figure 13**), which may slightly affect local stability; however, the overall binding remained energetically favorable. Structurally, the dominance of π-type interactions suggests that phenylalanine is well accommodated within a nonpolar region of TNF-α, where aromatic interactions are essential for ligand stabilization. This behavior aligns with the physicochemical properties of phenylalanine and supports its relatively strong docking performance. From a functional perspective, binding of phenylalanine to this region may influence the structural conformation of TNF-α or interfere with its interaction with receptors. Given the central role of TNF-α in inflammatory processes, such interactions may contribute to the suppression of inflammatory signaling pathways. Consequently, phenylalanine may play an important role in the overall anti-inflammatory activity of the As-Capsipol complex.

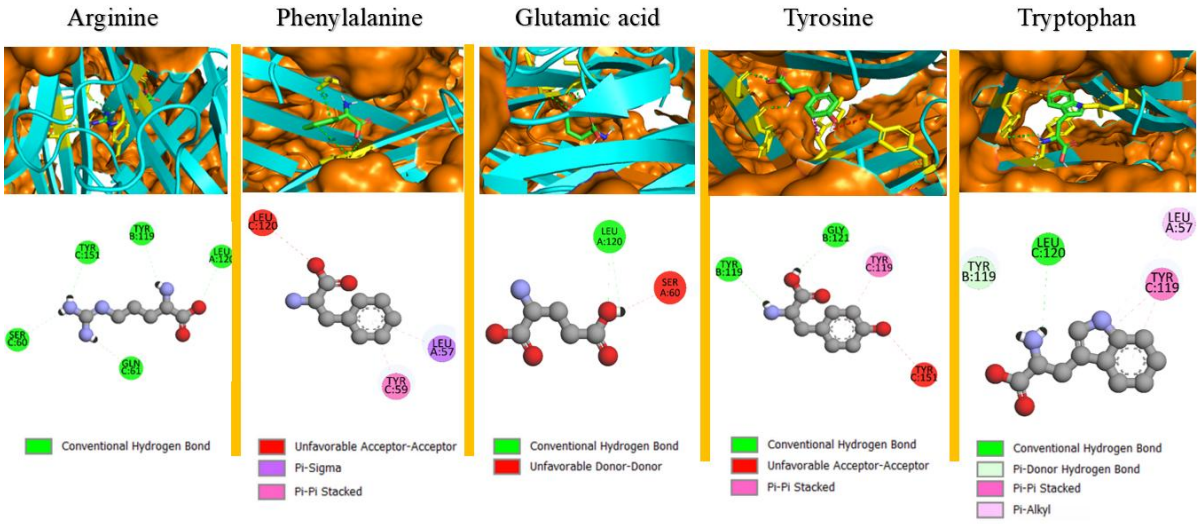


Figure 14 Comprehensive molecular docking visualization of selected As-Capsipol amino acids within the TNF alpha active site, illustrating binding modes, interaction networks, and structural alignment for arginine, phenylalanine, glutamine, tyrosine, and tryptophan.

Glutamic acid exhibited a binding affinity of −5.7 kcal/mol toward TNF-α (**Figure 13**), corresponding to an estimated Ki value of approximately 6.4×10^{-5} M (around 64 μM), which indicates a moderate inhibitory potential. Docking analysis shows that glutamic acid is accommodated within the binding region through conventional hydrogen bonding interactions, particularly with Leu120 (**Figure 14**). These interactions contribute to stabilizing the ligand within the protein environment. Given its negatively charged carboxylate groups, glutamic acid is well-suited for forming hydrogen bonds and electrostatic interactions with polar residues in the binding pocket. At the same time, an unfavorable donor–donor interaction was observed with Ser60, likely arising from repulsion between similarly oriented hydrogen donor groups. Although this interaction may slightly reduce local stability, it does not negate the overall favorable binding

energy of the complex. From a functional perspective, the binding of glutamic acid within this region may influence the structural conformation of TNF-α or partially interfere with its receptor-binding interface. Since TNF-α plays a central role in mediating inflammatory responses, such interactions could contribute to modulation of cytokine activity and attenuation of downstream inflammatory signaling.

Tyrosine demonstrated a binding affinity of −7.2 kcal/mol toward TNF-α, suggesting a relatively strong interaction within the active region of the protein. The docking simulation was carried out using a grid box centered at center_x = −42.604000, center_y = 96.193000, and center_z = 3.821000 (**Figure 13**), indicating that the ligand occupied a functionally significant site of TNF-α. Analysis of the interaction pattern revealed that tyrosine was stabilized by multiple contacts within the binding pocket. Conventional hydrogen bonds were formed with Gly121 and Tyr119 (**Figure 14**), contributing to stable anchoring of the ligand. Additionally, a π–π stacking interaction with Tyr119 further enhanced complex stability through aromatic interactions. An unfavorable acceptor–acceptor interaction with Tyr151 was also observed, which may slightly reduce local stability but does not significantly affect the overall binding affinity. From a structural standpoint, the combination of hydrogen bonding and aromatic interactions indicates that tyrosine fits well within a binding environment that includes both polar and hydrophobic features. The aromatic ring of tyrosine facilitates π-based interactions, while the hydroxyl group supports hydrogen bond formation, together promoting stable ligand accommodation. In terms of functional implications, the binding of tyrosine to this region may alter the conformational dynamics of TNF-α or interfere with its interaction with receptors. Given the important role of TNF-α in mediating inflammatory responses, such interactions may help reduce pro-inflammatory signaling. Therefore, tyrosine likely contributes significantly to the overall anti-inflammatory activity of the As-Capsipol complex.

Tryptophan exhibited a strong binding affinity of −8.1 kcal/mol toward TNF-α, corresponding to an estimated Ki value of approximately 1.1×10^{-6} M (around 1.1 μM), indicating a high inhibitory potential. The docking simulation was carried out using a grid box centered at center_x = −42.604000, center_y = 96.193000, and center_z = 3.821000 (**Figure 13**), confirming that the ligand occupies a structurally relevant region of the TNF-α target. Interaction analysis shows that tryptophan is stabilized within the binding pocket through a combination of hydrogen bonding and aromatic interactions. A conventional hydrogen bond with Leu120 contributes to anchoring the ligand (**Figure 14**), while π–π stacked interactions with Tyr119 and π–alkyl contacts with Leu57 further enhance stability. Additionally, a π-donor hydrogen bond involving Tyr119 supports proper ligand orientation within the pocket. The indole ring of tryptophan plays a crucial role in mediating these interactions, allowing efficient accommodation in a hydrophobic microenvironment. From a functional standpoint, binding of tryptophan at these coordinates may interfere with key structural or receptor-interacting regions of TNF-α. Given the role of TNF-α in pro-inflammatory signaling, such ligand binding could hinder receptor association and contribute to attenuation of downstream inflammatory responses.

Discussion

The present study demonstrates that the As-Capsipol complex exhibits hepatoprotective and anti-inflammatory activity, as supported by integrated in vivo and in silico analyses. Paracetamol-induced hepatotoxicity is widely associated with oxidative stress, depletion of glutathione, and accumulation of the reactive metabolite N-acetyl-p-benzoquinone imine, which leads to hepatocellular damage and necrosis. In the current study, administration of paracetamol resulted in significant liver injury, as evidenced by elevated ALT and AST levels and a reduction in urea concentration, indicating impaired hepatocyte integrity and metabolic function. Treatment with As-Capsipol was associated with improvement in these biochemical parameters, including a reduction in transaminase levels and partial restoration of urea concentration. These findings suggest stabilization of hepatocellular membranes and a degree of recovery in liver metabolic activity. The observed effects may be related to the presence of bioactive components within the complex, which could contribute to modulation of oxidative and inflammatory processes involved in liver injury. The anti-inflammatory activity of As-Capsipol was further confirmed using the carrageenan-induced paw edema model. In this model, maximal edema was observed at 3

h in the control group, whereas treatment with As-Capsipol reduced the degree of swelling in a dose-dependent manner. The highest anti-exudative activity was observed at a dose of 150 mg/kg, with a noticeable attenuation of edema compared to the untreated group. These results indicate that As-Capsipol may interfere with the development of acute inflammatory responses, particularly during the exudative phase. In addition, the acute toxicity assessment demonstrated that oral administration of As-Capsipol at a dose of 2,000 mg/kg did not result in mortality or persistent toxic effects in mice. Although transient behavioral changes were observed shortly after administration, these effects were reversible and did not influence overall physiological status or body weight gain during the observation period. Based on these findings, the median lethal dose (LD50) can be considered to exceed 2,000 mg/kg, indicating a low level of acute toxicity under the tested conditions. The molecular docking analysis provided further insight into the potential mechanisms underlying the observed biological effects. The selected amino acids showed favorable binding affinities toward key inflammatory targets, including MAPK, NF-kB, and TNF-α. Among the investigated ligands, tryptophan exhibited the strongest interactions, followed by tyrosine and phenylalanine, while arginine and glutamic acid demonstrated moderate binding. These interactions were supported by hydrogen bonding, hydrophobic contacts, and π–π interactions within the active sites of the proteins, suggesting the potential to influence key signaling pathways involved in inflammation. The consistency between experimental and computational findings supports the assumption that the biological activity of As-Capsipol may involve a multi-target mechanism associated with modulation of inflammatory processes. However, it should be noted that the present study is limited to experimental and modeling approaches. Further investigations, including detailed molecular and histological analyses, are required to more clearly define the mechanisms of action and to evaluate the potential applicability of As-Capsipol in broader biomedical contexts.

Conclusions

The findings of the present study indicate that the As-Capsipol complex demonstrates hepatoprotective and anti-inflammatory potential under experimental conditions. In the paracetamol-induced hepatitis model, administration of As-Capsipol was associated with improvement in key biochemical markers, including reductions in ALT and AST levels and partial restoration of urea concentration, suggesting recovery of hepatocyte integrity and metabolic function. In the carrageenan-induced inflammation model, the compound exhibited dose-dependent anti-exudative activity, with higher doses showing greater attenuation of edema formation. The acute toxicity assessment further indicated that As-Capsipol did not produce mortality or persistent adverse effects at a dose of 2,000 mg/kg, suggesting a low level of acute toxicity within the tested range. Molecular docking analysis supported these experimental findings by demonstrating that selected amino acid components of the complex can interact with key inflammation-related targets, including MAPK, NF-kB, and TNF-α. The observed binding affinity pattern (Tryptophan > Tyrosine ≈ Phenylalanine > Arginine > Glutamic acid) suggests a potential role of aromatic amino acids in mediating ligand–protein interactions. Overall, the combined *in vivo* and in silico results suggest that the biological activity of the As-Capsipol complex may involve a multi-target mechanism associated with modulation of inflammatory processes and liver function. However, these findings are limited to experimental and computational models, and further studies, including detailed mechanistic and clinical investigations, are necessary to more clearly define its potential applications.\

Acknowledgments

We have no grant and we also would like to thanks for Science Academy of Uzbekistan for their great contributions. This research was funded by the international project No. AL-FDU2022307-004, entitled “Development and production of therapeutic products from fruit waste generated in agriculture,” for the period 2022-2026.

Declaration of generative AI in scientific writing

The authors acknowledge the use of generative AI tools for language editing and grammar correction. No content generation or data interpretation was performed by AI. The authors take full responsibility for the content and conclusions of this work.

CRediT author statement

Baxtigul Obidova Ro'zmat Qizi: Investigation, Methodology, Data Curation, Formal Analysis, Writing - Original Draft, Laboratory Experiments, Data Collection; **Ibragim Raxmanovich Askarov**: Conceptualization, Supervision, Project Administration, Writing - Review & Editing; **Surayyo Mamatqulova Abdusamatovna**: Validation, Resources, Literature Review, Reference Management, Writing - Review & Editing; **Muzaffar Obidov**: Literature Review, Reference Management, Writing - Review & Editing.

Declaration of competing interest

The authors declare that they have no known competing financial interests or personal relationships that could have appeared to influence the work reported in this paper.

Reference

[1] SA Ali, NH Sharief and YS Mohamed. Hepatoprotective activity of some medicinal plants in Sudan. *Evidence-Based Complementary and Alternative Medicine* 2019; **2019**, 2196315.

[2] P Liu, W Chen, D Wu, Z Zhang, W Li and Y Yang. The preparation, modification and hepatoprotective activity of chitooligosaccharides: A review. *International Journal of Biological Macromolecules* 2024; **277**, 134489.

[3] DS Mandlik and AG Namdeo. Pharmacological evaluation of Ashwagandha highlighting its healthcare claims, safety, and toxicity aspects. *Journal of Dietary Supplements* 2021; **18(2)**, 183-226.

[4] J Deng, Y Cong, X Han, W Wei, Y Lu, T Liu, W Zhao, B Lin, Y Luo and X Zhang. A liver-on-a-chip for hepatoprotective activity assessment. *Biomicrofluidics* 2020; **14(6)**, 064107.

[5] S He, Y Yi, D Hou, X Fu, J Zhang, X Ru, J Xie and J Wang. Identification of hepatoprotective traditional Chinese medicines based on the structure–activity relationship, molecular network, and machine learning techniques. *Frontiers in Pharmacology* 2022; **13**, 969979.

[6] DH Lee, JS Park, LY S, J Han, DK Lee, SW Kwon, DH Han, YH Lee and SH Bae. SQSTM1/p62 activates NFE2L2/NRF2 via ULK1-mediated autophagic KEAP1 degradation and protects mouse liver from lipotoxicity. *Autophagy* 2020; **16(11)**, 1949-1973.

[7] QD Le, HD Vu, VM Nguyen, GJ Choi, LTP Hoa, DT Dung, PV Kiem, NX Nhiem, QD De, QC Nguyen, DT Nghiem and DN Quang. Desmodinosides A-E: New flavonoid C-glycosides from *Desmodium heterocarpon* var. *strigosum* with hepatoprotective and antifungal activity. *Fitoterapia* 2023; **169**, 105609.

[8] BD Hiraganahalli, VC Chinampudur, S Dethe, D Mundkinajeddu, MK Pandre, J Balachandran and A Agarwal. Hepatoprotective and antioxidant activity of standardized herbal extracts. *Pharmacognosy Magazine* 2012; **8(30)**, 116-123.

[9] C Zhao, J Fan, Y Liu, W Guo, H Cao, J Xiao, Y Wang and Liu B. Hepatoprotective activity of *Ganoderma lucidum* triterpenoids in alcohol-induced liver injury in mice, an iTRAQ-based proteomic analysis. *Food Chemistry* 2019; **271**, 148-156.

[10] M Iranshahy, M Iranshahi, SR Abtahi and G Karimi. The role of nuclear factor erythroid 2-related factor 2 in hepatoprotective activity of natural products: A review. *Food and Chemical Toxicology* 2018; **120**, 261-276.

[11] T Lan, Y Yu, J Zhang, H Li, Q Weng, S Jiang, S Tian, T Xu, S Hu, G Yang, Y Zhang, W Wang, L Wang, Q Zhu, X Rong and J Guo. Cordycepin ameliorates nonalcoholic steatohepatitis by activation of the AMP-activated protein kinase signaling pathway. *Hepatology* 2021; **74(2)**, 686-703.

[12] Putz P, Klinger M, Male C, Pabinger I. Lower physical activity and altered body composition in patients with haemophilia compared with healthy controls. Haemophilia. 2021 Mar;27(2):e260-e266. doi: 10.1111/hae.14259. Epub 2021 Feb 12. PMID: 33578451; PMCID: PMC8048548

[13] .A Hermenean, T Mariasiu, I Navarro-González, J Vegara-Meseguer, E Miuțescu, S Chakraborty and H Pérez-Sánchez. Hepatoprotective activity of chrysin is mediated through TNF-α in chemically-induced acute liver damage: An *in vivo* study and molecular modeling. *Experimental and Therapeutic Medicine* 2017; **13(5)**, 1671-1680.

[14] Hoffman RP. Sympathetic mechanisms of hypoglycemic counterregulation. Curr Diabetes

Rev. 2007 Aug;3(3):185-93. doi: 10.2174/157339907781368995. PMID: 18220670.V Kaur, M Kumar, P Kaur, S Kaur, AP Singh and S Kaur. Hepatoprotective activity of *Butea monosperma* bark against thioacetamide-induced liver injury in rats. *Biomedicine & Pharmacotherapy* 2017; **89**, 332-341.

[15] K Lahon and S Das. Hepatoprotective activity of *Ocimum sanctum* alcoholic leaf extract against paracetamol-induced liver damage in Albino rats. *Pharmacognosy Research* 2011; **3(1)**, 13-18.

[16] P Niziński, A Krajewska, T Oniszczuk, B Polak and A Oniszczuk. Hepatoprotective effect of kaempferol - A review. *Molecules* 2025; **30(9)**, 1913.

[17] HS Park, E Jo, JH Han, SH Jung, DH Lee, I Park, KS Heo, M Na and CS Myung. Hepatoprotective effects of an *Acer tegmentosum* Maxim extract through antioxidant activity and the regulation of autophagy. *Journal of Ethnopharmacology* 2019; **239**, 111912.

[18] Z Meena, MA Rahman, P Bagga and M Mujahid. Hepatoprotective activity of *Tamarindus indica* Linn stem bark ethanolic extract against hepatic damage induced by co-administration of antitubercular drugs isoniazid and rifampicin in Sprague Dawley rats. *Journal of Basic and Clinical Physiology and Pharmacology* 2018; **30(1)**, 131-137.

[19] NT Selvam, V Venkatakrishnan, R Dhamodharan, S Murugesan and SD Kumar. Hepatoprotective activity of methanolic extract of *Syzygium jambos* (Linn.) leaf against paracetamol intoxicated Wistar albino rats. *Ayu* 2013; **34(3)**, 305-308.

[20] R Domitrović and I Potočnjak. A comprehensive overview of hepatoprotective natural compounds: mechanism of action and clinical perspectives. *Archives of Toxicology* 2016; **90(1)**, 39-79.

[21] DZ Xia, PH Zhang, Y Fu, WF Yu and MT Ju. Hepatoprotective activity of puerarin against carbon tetrachloride-induced injuries in rats: A randomized controlled trial. *Food and Chemical Toxicology* 2013; **59**, 90-95.

[22] AR Rao, R Sarada, MD Shylaja and GA Ravishankar. Evaluation of hepatoprotective and antioxidant activity of astaxanthin and astaxanthin esters from microalga - *Haematococcus pluvialis*. *Journal of Food Science and Technology* 2015; **52(1)**, 6703-6710.

[23] X Su, L Li, H Sun, Z Zhang, C Li, F Li, H Wang, B Li, R Chen and J Kang. Eight new glycosides with hepatoprotective activity isolated from the aerial parts of *Morinda parvifolia*. *Bioorganic Chemistry* 2019; **87**, 867-875.

[24] HA Mohammed, HM Eldeeb, RA Khan, MS Al-Omar, SAA Mohammed, MSM Sajid, MSA Aly, AM Ahmad, AAH Abdellatif, SY Eid and MZ El-Readi. Sage, *Salvia officinalis* L., constituents, hepatoprotective activity, and cytotoxicity evaluations of the essential oils obtained from fresh and differently timed dried herbs: A comparative Analysis. *Molecules* 2021; **26(19)**, 5757.

[25] L Pinzi and G Rastelli. Molecular docking: Shifting paradigms in drug discovery. *International Journal of Molecular Sciences* 2019; **20(18)**, 4331.

[26] LG Ferreira, RN Dos Santos, G Oliva and AD Andricopulo. Molecular docking and structure-based drug design strategies. *Molecules* 2015; **20(7)**, 13384-13421.

[27] A Bisht, D Tewari, S Kumar and S Chandra. Network pharmacology, molecular docking, and molecular dynamics simulation to elucidate the mechanism of anti-aging action of *Tinospora cordifolia*. *Molecular Diversity* 2024; **28(3)**, 1743-1763.

[28] K Crampon, A Giorkallos, M Deldossi, S Baud and LA Steffenel. Machine-learning methods for ligand-protein molecular docking. *Drug Discovery Today* 2022; **27(1)**, 151-164.

[29] F Stanzione, I Giangreco and JC Cole. Use of molecular docking computational tools in drug discovery. *Progress in Medicinal Chemistry* 2021; **60**, 273-343.

[30] T Li, R Guo, Q Zong and G Ling. Application of molecular docking in elaborating molecular mechanisms and interactions of supramolecular cyclodextrin. *Carbohydrate Polymers* 2022; **276**, 118644.

[31] Y Hou, Y Bai, C Lu, Q Wang, Z Wang, J Gao and H Xu. Applying molecular docking to pesticides. *Pest Management Science* 2023; **79(11)**, 4140-4152.

[32] LHS Santos, RS Ferreira and ER Caffarena. Integrating Molecular Docking and Molecular Dynamics Simulations. *Methods in Molecular Biology* 2019; **2053**, 13-34.

[33] J Wang, Y Bai, X Guan, Y Lao and Z Dong. Network pharmacology and molecular docking study on the mechanism of chronic prostatitis treatment using Xiaochaihutang. *Asian Journal of Surgery* 2023; **46(11)**, 4798-4800.

[34] S Baghaki, CE Yalcin, HS Baghaki, SY Aydin, B Daghan and E Yavuz. COX-2 inhibition in the treatment of COVID-19: Review of literature to propose repositioning of celecoxib for randomized controlled studies. *International Journal of Infectious Diseases* 2020; **101**, 29-32.

[35] M Lyndin, O Kravtsova, K Sikora, Y Lyndina, Y Kuzenko, WA Awuah, T Abdul-Rahman, N Hyriavenko, V Sikora and A Romaniuk. COX-2 effects on endometrial carcinomas progression. *Pathology - Research and Practice* 2022; **238**, 154082.

[36] D Barrett. IL-6 blockade in cytokine storm syndromes. *Advances in Experimental Medicine and Biology* 2024; **1448**, 565-572.

[37] T Tanaka, M Narazaki, K Masuda and T Kishimoto. Regulation of IL-6 in immunity and diseases. *Advances in Experimental Medicine and Biology* 2016; **941**, 79-88.

[38] YJ Guo, WW Pan, SB Liu, ZF Shen, Y Xu and LL Hu. ERK/MAPK signalling pathway and tumorigenesis. *Experimental and Therapeutic Medicine* 2020; **19(3)**, 1997-2007.

[39] L Kalvaitis, G Gedvilaite-Vaicechauskiene, L Kriauciuniene and R Liutkeviciene. TNF-alfa gene polymorphism associations with multiple sclerosis. *Journal of Clinical Medicine* 2024; **13(13)**, 3693.

[40] S Kochbati, F Boussema, MB Miled, S Ktari, L Daoud, SB Rhouma, GB Amor, O Chérif and L Rokbani. Les modulateurs du TNFalpha dans le traitement de la polyarthrite rhumatoide. *Tunisie Medicale* 2004; **82(10)**, 893-904.